AFFDL-TR-79-3089

APA 082030

DEVELOPMENT OF RECORDING MATERIALS FOR HOLOGRAPHIC
NONDESTRUCTIVE TESTING

A. A. Friesem
S. Reich

Weizmann Institute of Science
Rehovot, Israel

August 1979

TECHNICAL REPORT AFFDL-TR-79-3089

Final Report for Period 1 June 1976 - 31 May 1977 and 1 Sep 1977 - 31 Aug 1978

Approved for public release; distribution unlimited

20070925187

AIR FORCE FLIGHT DYNAMICS LABORATORY
AIR FORCE WRIGHT AERONAUTICAL LABORATORIES
AIR FORCE SYSTEMS COMMAND
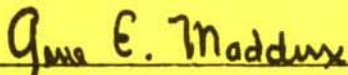WRIGHT-PATTERSON AIR FORCE BASE, OHIO 45433

Gene E. Maddux
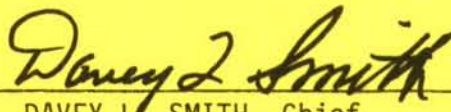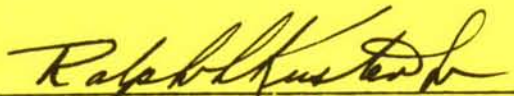Project Engineer

DAVEY L. SMITH, Chief
Structural Integrity Branch
Structures & Dynamics Division

FOR THE COMMANDER

RALPH L. KUSTER, JR, Col, USAF
Chief, Structures & Dynamics Division
Flight Dynamics Laboratory (AFWAL)

REPORT DOCUMENTATION PAGE		READ INSTRUCTIONS BEFORE COMPLETING FORM
1. REPORT NUMBER AFFDL-TR-79-3089	2. GOVT ACCESSION NO.	3. RECIPIENT'S CATALOG NUMBER
4. TITLE (and Subtitle) Development of Recording Materials for Holographic Non-Destructive Testing		5. TYPE OF REPORT & PERIOD COVERED Final Report 1 June 1976-31 May 1977, 1 Sep 1977-30 Aug 1978
		6. PERFORMING ORG. REPORT NUMBER
7. AUTHOR(s) A. A. Friesem and S. Reich		8. CONTRACT OR GRANT NUMBER(s) AFOSR-77-3421 AFOSR-76-3004
9. PERFORMING ORGANIZATION NAME AND ADDRESS Weizmann Institute of Science, Rehovot, Israel		10. PROGRAM ELEMENT, PROJECT, TASK AREA & WORK UNIT NUMBERS 61102F 2307N108
11. CONTROLLING OFFICE NAME AND ADDRESS		12. REPORT DATE August 1979
		13. NUMBER OF PAGES
14. MONITORING AGENCY NAME & ADDRESS(if different from Controlling Office) AFWAL/AFFDL/FBE Wright-Patterson AFB, Ohio 45433		15. SECURITY CLASS. (of this report)
		15a. DECLASSIFICATION/DOWNGRADING SCHEDULE

16. DISTRIBUTION STATEMENT (of this Report)

Approved from public release; distribution unlimited.

17. DISTRIBUTION STATEMENT (of the abstract entered in Block 20, if different from Report)

18. SUPPLEMENTARY NOTES

19. KEY WORDS (Continue on reverse side if necessary and identify by block number)

Recording Materials; Holographic Non-Destructive Testing; Hologram Interferometry

20. ABSTRACT (Continue on reverse side if necessary and identify by block number)

This report describes a two year effort on investigating two recording materials for in-situ, real-time holographic nondestructive field testing application, namely, photodielectrics and photoconductorthermoplastic devices (PC-TP).

The holographic parameters as well as the recording mechanism of photo-dielectric materials were thoroughly studied. The recording mechanism is attributed to photochemically induced cross links of macromolecules. Resolution on excess of 2500 1/mm and diffraction efficiency approaching 100% were measured. Due to the

DD FORM 1473 1 JAN 73   EDITION OF 1 NOV 65 IS OBSOLETE

low exposure sensitivity, about 1 J/cm^2, this recording material could only be incorporated into systems for testing relatively small objects.

A number of ways for operating the PC-TP devices more reliably and for improving the spatial bandwidth to over 1800 1/mm were established. Furthermore, the frost formation mechanism was investigated, and means for supressing the frost were determined, thereby leading to improved signal-to-noise ratio. These results together with the high exposure sensitivity (50 erg/cm^2) and the improvements in sample fabrication, have led to an operable device which may be incorporated into most holographic non-destructive systems.

FOREWORD

This final report covers work performed between 1 June 1976 to 31 May 1977, and 1 Sep 1977 to 31 Aug 1978. The effort was sponsored by the Structural Integrity Branch, Structures and Dynamics Division, Air Force Flight Dynamics Laboratory, Wright-Patterson AFB, OH 45433 under grant AFOSR-76-3004, Project 2307, Work Unit 2307N108. The grant was administered by G. E. Maddux. The principal investigators are A. A. Friesem and S. Reich. Other majro contributors to the effort are Z. Rav-Noy, Y. Katzir and B. Sharon.

TABLE OF CONTENTS

LIST OF FIGURES

1. INTRODUCTION

One of the earliest and still viable major applications of holography is hologram interferometry. The underlying principle is that the reconstructed image duplicates the original object in amplitude and phase resulting in duplication so precise that the reconstructed image and the actual object fuse together and appear as one. The reconstructed image may therefore be substituted for the actual object in an interferometric application, for instance, by using the reconstructed image as a "standard" to test similar objects. Also, the reconstructed image and actual object can be interfered against each other, thus allowing for sensitive detection of a difference in distance or index of refraction. This technique is being used effectively in non-destructive measurements of vibrations, stress, strain, as well as for the detection of cracks and fissures[1-4]. Concrete examples include the identification of fatigue failure in aircraft wings; the detection of "disbonds" in multilayered materials such as tiles and honey-comb structures; the determination of heat stresses in laser rods; and the study of the dynamic operation of audio speakers and stringed musical instruments.

Predictions of the widespread industrial application of interferometry have not yet been realised. The technique requires extreme accuracy in set-up and is far more sensitive than necessary for most industrial non-destructive testing of mass-produced items. But as the industrial sophistication increases (computer components, satellites , aircraft, miniaturized electronic

instruments), hologram interferometry may prove a highly suitable method, entirely competitive with standard techniques such as X-rays and ultrasonic analysis.

Yet, there remains a major obstacle which is the lack of suitable material to record in-situ and in real time the necessary hologram. The most commonly used recording material is the photographic emulsion with its attendant difficulties of time consuming wet processing for development. Although many other materials which can be developed in virtually real time have been used or suggested for holographic recordings, only photoconductor-thermoplastic (PC-TP) devices and the more recently developed photodielectric polymers possess most of the desired characteristics necessary for holographic non-destructive applications - relatively good exposure sensitivity, noise characteristics and diffraction efficiency, virtually real time and in-situ development, and capability of permanent storage.

The recording materials have been extensively studied by us in the past, but the emphasis has generally been on determining their usefulness in high density holographic storage and retrieval applications. Relatively little attention has been given to the study of these materials for use in holographic non-destructive testing.

The objective of this two year research was to further develop these recording materials and enhance their holographic response, so that

they could be incorporated into a holographic non-destructive testing (HNDT) system.

Our efforts have led to a prototype of a photoconductor-thermoplastic recording system, which satisfies most HNDT requirements. The photodielectrics on the other hand are not as attractive for HNDT because of their low exposure sensitivity; as a consequence they are confined to testing relatively small objects.

2. PHOTODIELECTRIC MATERIALS

2.1 General

With the growth of modern holography there has been considerable interest in thick phase recording materials. The interest in these materials, most of which are polymers offering _in situ_ development mechanism, is due primarily to their high density storage capabilities, high diffraction efficiencies and excellent noise characteristics. The best known examples of polymeric materials include: (1) the polymethylmethacrylate (PMMA) sensitive in the UV range [5-7], in which the recording is reported to be due to either photoinduced crosslinking [5], or due to polymerization of residual monomer [7]; (2) the PMMA sensitized for the blue-green visible range in which the recording is attributed to photodegradation [8] or to crosslinking [9], (3) the polymer sensitized with diketones in which the recording is due to either inter or intra molecular hydrogen abstraction [10]; (4) the photopolymers in which the recording is due to photopolymerization of monomers [11-13]; and (5) the more recent multicomponent photopolymer systems in which the recording is due to polymerization of monomers accompanied by phase separation [14].

Most of these materials, unfortunately have a short shelf-life and require relatively complex preparation procedure in order to achieve high optical quality recording areas. In this report we describe a newly developed polymeric material which is relatively easy to prepare possesses, long shelf-life, and yet exhibits holographic response comparable to the other materials.

The results presented here indicate that the recording mechanism is due to refractive index modulation resulting from an increase in density.

This density increase appears to be caused by crosslinking and not by photopolymerization as reported for some other similar materials.

2.2. Material and Sample Preparation

The recording material is a polymeric system comprised of poly (methyl α-cyanoacrylate) sensitized with parabenzoquinone (PBQ). To prepare this we begin with the monomer which is obtained by depolymerization [15]. The parabenzoquinone sensitizer, suitably purified by a sublimation process, is then introduced into the monomer and the resulting solution is polymerized between glass plates or between other equivalent substrate materials. In general these substrates need not be specially treated. Thicknesses ranging from a few microns to several millimeters can be obtained by merely placing appropriate spacers between glass plates.

The methylα-cyanoacrylate monomers are highly reactive and they polymerize both by free radical initiation and by anionic initiation. In large bulk form, the polymerization is inhibited by the introduction of quinone sensitizer. However, for large ratios of surface area to volume, anionic initiation is dominant and polymerization occurs rapidly. For example, thin plates of about 50 microns thickness and areas greater than 1 cm^2 can be prepared in several minutes, whereas plates of 200 microns thickness can be prepared in about one hour.

When polymerization occurs, the excellent bonding and filling properties of the cyanoacrylate allow for the formation of an exact replica of the glass substrates, so that high optical quality can be achieved. Furthermore, the volume of the photodielectric material remains constant during the polymerization process [16]. After polymerization is completed the substrates could be removed and the hard surface of the material polished to any desired surface quality.

An important advantage in the preparation of these materials is that no solvent is needed to introduce the sensitizers into the polymer. Thus the slow evaporation ususally necessary in preparing conventional photodielectric materials is avoided, resulting in excellent optical quality. The plasticizing action of the solvent on a polymer tends to degrade its dimensional stability; also when it reacts with the sensitizer, the solvent degrades the sensitivity of the materials. Eliminating the solvent, thus makes it possible to obtain improved dimensional and chemical properties, resulting in increased shelf life. In our experiments, high quality holograms were recorded with polymerized samples that had been stored for over twelve months.

2.3. Holographic Response

We performed a series of experiments to determine the exposure sensitivity, resolution, diffraction efficiency and signal-to-average noise ratio of various photodielectric material samples.

To measure the exposure sensitivity, resolution, and diffraction efficiency, we recorded simple interference gratings by using plane waves for both reference and signal beam. For the experiments we varied the average exposure, the reference-to-signal beam ratio, thickness of recording medium, spatial frequency and sensitizer concentration. In readout we measured the diffracted laser beam power P_d, the incident beam power P_i, and the power transmitted by the unexposed portion of the material, P_t; during the measurements we noted a slight bleaching effect at the exposed regions, but it was too small, to significantly affect the value of P_t. Generally, the value of P_t ranged from 70 percent to 90 percent of the incident beam power, depending on thicknesses and sensitizer concentration of the samples as well as on the incidence angle and wavelength of the readout beam. For example, the absorption coefficients, with sensitizer concentrations of 7 percent, were $11 cm^{-1}$ at 488nm, and $2.4 cm^{-1}$ at 632.8nm. The diffraction efficiency, defined as the ratio of the average diffracted power to the transmitted power, was then calculated from the measured values.

Since the spectral response of the quinone-sensitized photodielectric materials is limited to the blue-green region of the visible spectrum, it was advantageous to use the recording-readout arrangement shown schematically in Fig. 1, where the recording and readout parameters can be simultaneously measured. The recording wavelength of 488 nm was from an argon laser, and the readout wavelength of 632.8 nm was from a he-ne laser. The angle of incidence of the readout beam, θ_2,

Recording

Plane Waves
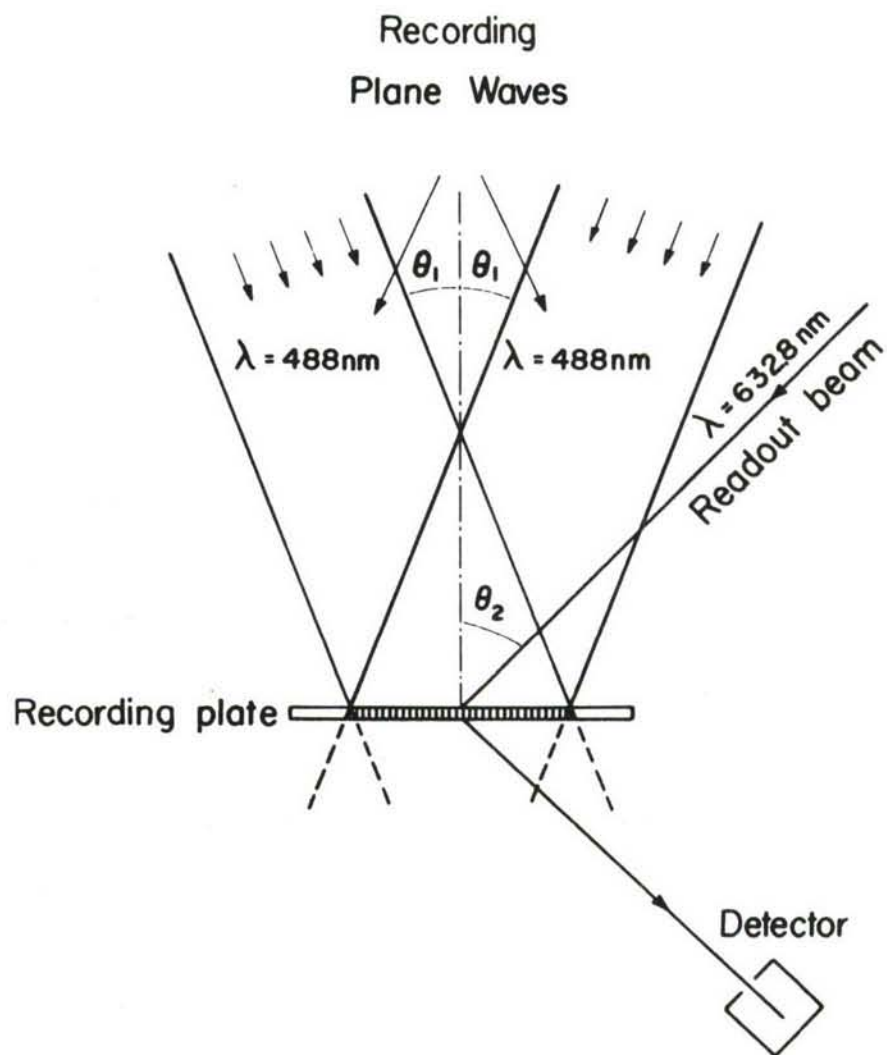
Figure 1. Recording-readout arrangement.

is adjusted to satisfy the Bragg condition in order to obtain maximum diffraction. This angle is related to the recording angles θ_1, by the relation $\theta_2 = \sin^{-1}[\frac{\lambda_2}{\lambda_1} \sin \theta_1]$, where λ_1 and λ_2 are the recording and readout wavelengths respectively. By employing a photodetector to monitor the diffracted power and a storage oscilloscope, the behavior of the photodielectrics can be studied.

The oscilloscope tracings shown in Fig. 2 depict typical results from the arrangement of Fig. 1. In the photograph shown in Fig. 2(a), the rectangular trace depicts the recording pulse of the reference beam and the rising trace represents the diffracted power, both given as a function ot exposure time. Shortly after the initiation of exposure, the diffraction begins and continues to rise while the recording is going on. The diffracted power continues to increase even after the exposure pulse is terminated; we attribute this additional increase to the continual propagation of the photochemical reaction in the material, which continues until a steady state level in diffracted power is reached. If the exposure continues we obtain the results of Fig. 2(b) which shows several sweeps of the oscilloscope depicting the diffracted power only as a function of exposure time. In sweep 1, the diffracted power rises to a maximum value and as the recorded grating is overmodulated the diffracted power begins to decrease. This decrease continues as depicted by sweep 2, and then begins to rise again in sweep 3 and subsequent sweeps until the material saturates in sweep 6. This type of overmodulated diffraction were obtained only with the relatively thick samples whose thicknesses were greater than 100 microns.
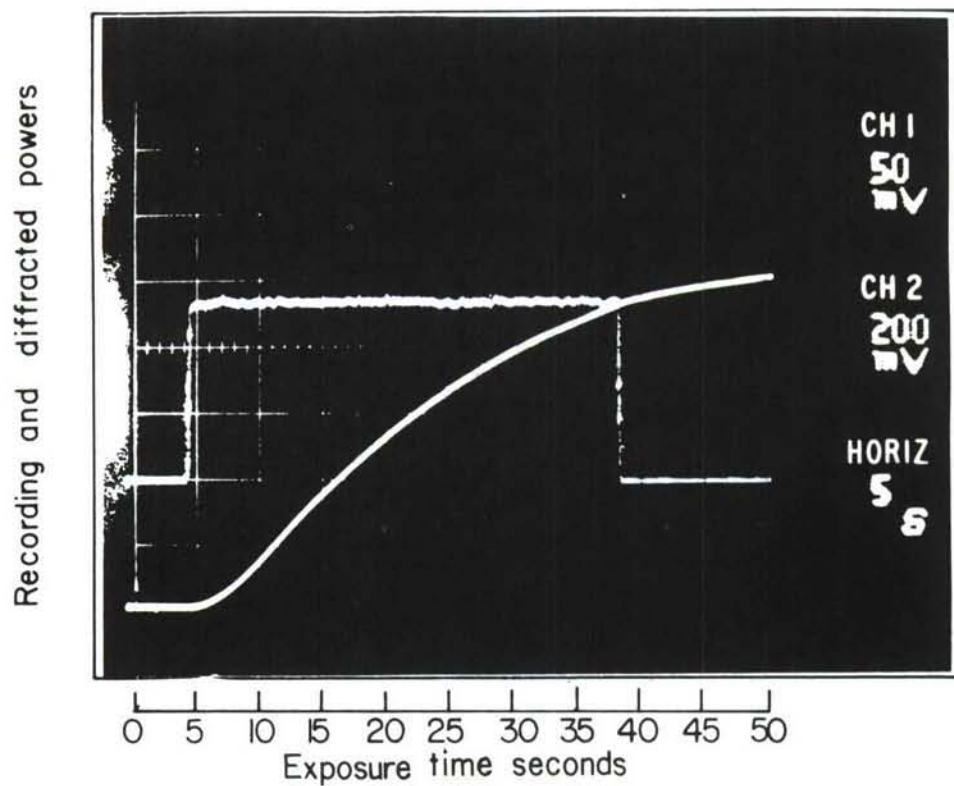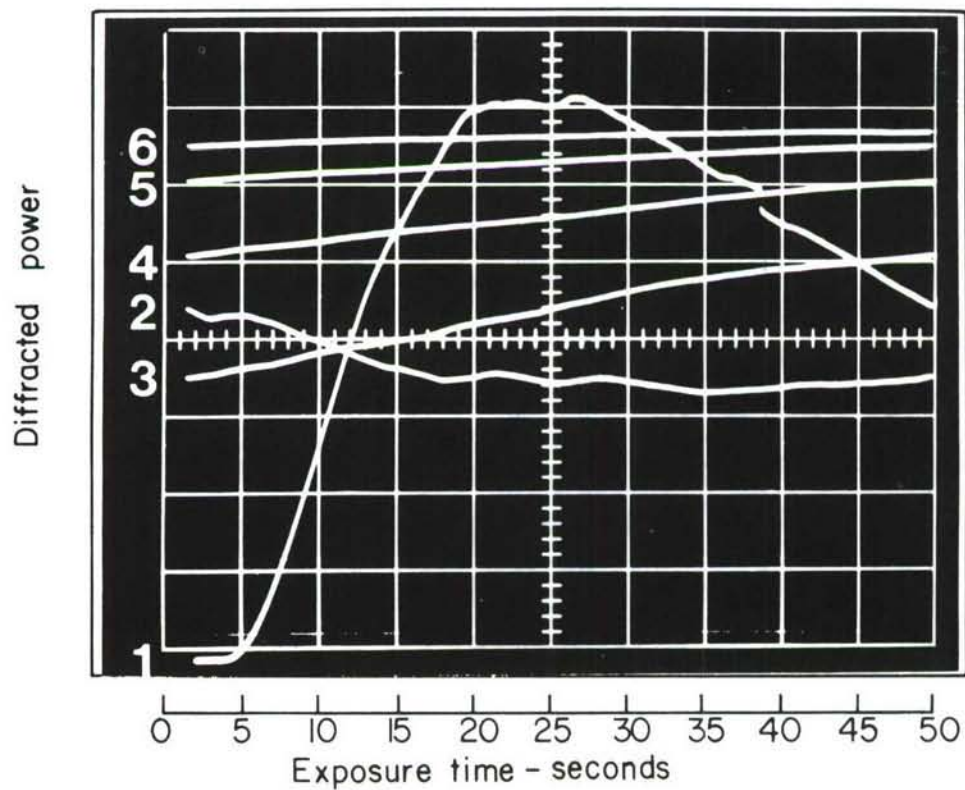
Figure 2. Dynamic behavior traces of diffracted and recording intensities.

(a) Typical behavior

(b) Showing over modulation.

As the thicknesses of the recording layers increase beyond 200 microns, the experimental arrangement shown in Fig. 1 ceases to be suitable for obtaining quantitative values of diffracted power since the angular orientation of the readout beam becomes overly critical. An alternative arrangement for simultaneously monitoring the recording and readout is to chop one of the recording beam so that the detector alternately monitors the power of the direct recording beam or the diffracted beam. A typical result from such an arrangement is shown in the oscillograph tracings of Fig. 3. The upper trace is the direct recording beam which is relatively constant, whereas the lower trace depicts the diffracted power which increases as a function of exposure time.

The quantitative results from such oscillograph traces are shown in Figs. 4 and 5. Figure 4 shows diffraction efficiency as a function of exposure for three different polymer samples each of a different thickness. The reference-to-signal beam ratio was 2:1, the recorded spatial frequency was 1000 lines/mm the combined average exposure intensity of the two beam was about 100mW, and the PBQ sensitizer concentration was 7 percent. As expected, the exposure level necessary to reach high diffraction efficiencies is lower for the thicker samples. By varying the recording angles we determined that the photodielectrics have high resolving capabilities; we found from the transmission hologram measurements that the response is fairly constant from spatial frequencies of 100 lines/mm to spatial frequencies exceeding 2000 lines/mm.

We noted that when recording holographic gratings in very thick samples, the materials become cloudy at high exposure levels. This cloudiness is probably due to a cooperative noise formation in the volume of the material
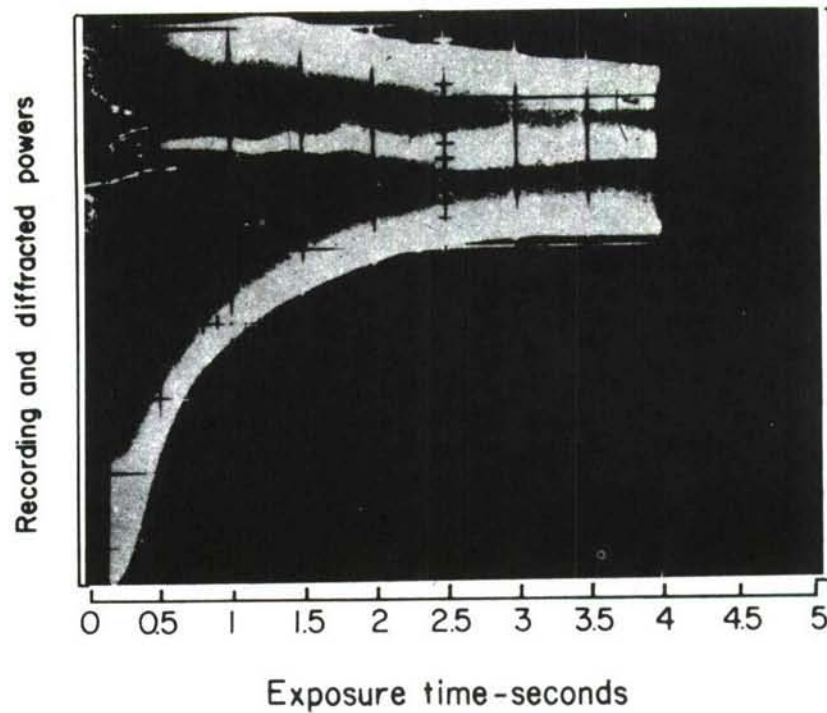
Figure 3.   Traces of very thick recording layers.
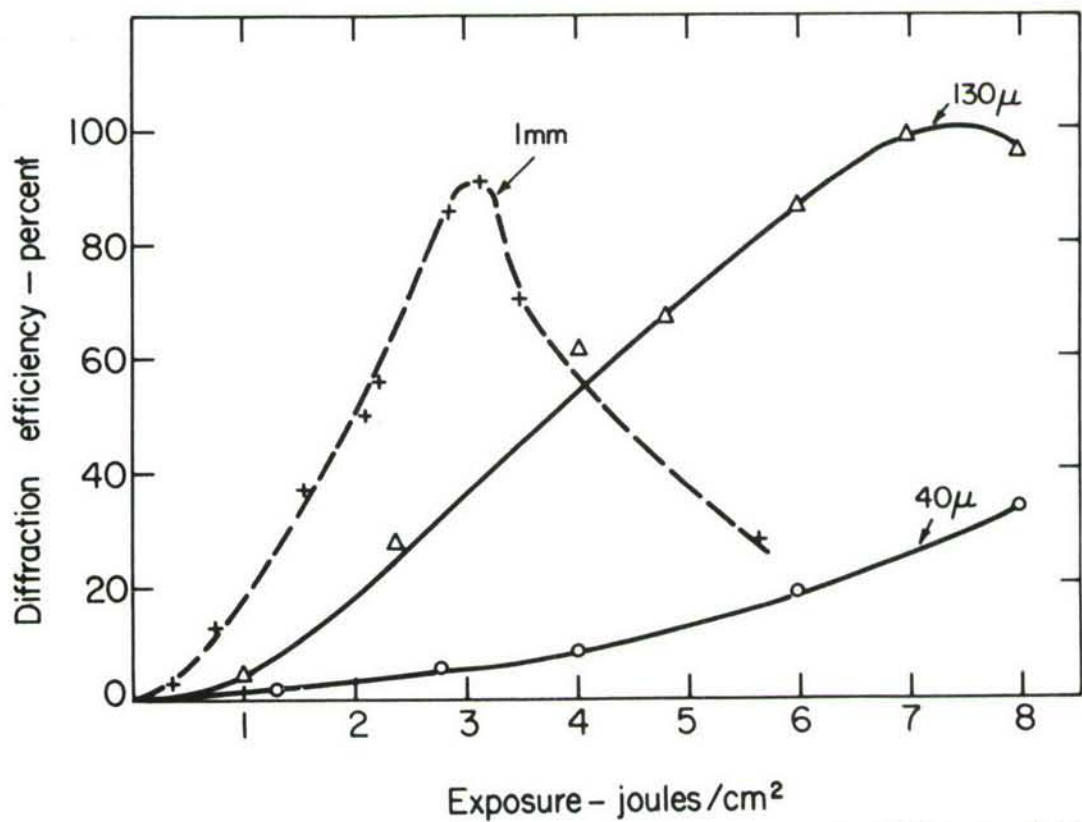
Figure 4.   Diffraction efficiency as a function of exposure for different thicknesses.

when the density of the cross links forming the hologram is excessive; this tends to degrade the response of the holographic grating. Consequently care must be taken not to overexpose the thick samples.

Figure 5 shows the effect of sensitizer concentration on the holographic response. To obtain this data several samples of equal thickness, each having a different concentration of sensitizers (PBQ), were selected for recording simple holographic gratings; the recording parameters such as offset angle, reference-to signal beam intensity ratio, and exposure levels were maintained constant. As shown in Fig. 5, the diffraction efficiency increases to reach a maximum value at a sensitizer concentration of about 8 percent. Beyond this concentration value the diffraction decreases - probably due to dimerization of the sensitizer [17].

We also noted that the temporal stability of the recorded hologram is a function of the initial diffraction efficiencies. As shown in the results of Fig. 6, the diffraction efficiencies for simple holographic gratings in 100 microns thick samples remain constant if the initial efficiencies are greater than 90 percent; in this case the index modulation is near maximum so that most of the benzoquinone is utilized. However, if the index modulation and consequently the initial diffraction efficiencies are relatively low, the efficiencies decrease during the first two days after recording; thereafter the holograms stabilize but with a lower diffraction efficiency. Between measurements the samples were left in the open under normal room temperature and light conditions. The holograms could be fixed with a uniform post exposure by an illumination beam of $100mW/cm^2$ at $\lambda=488nm$ for about one hour.

To measure the signal-to-average noise ratio, SNR, we recorded Fresnel holograms of a diffusely illuminated data mask consisting of a square with an

- 13 -
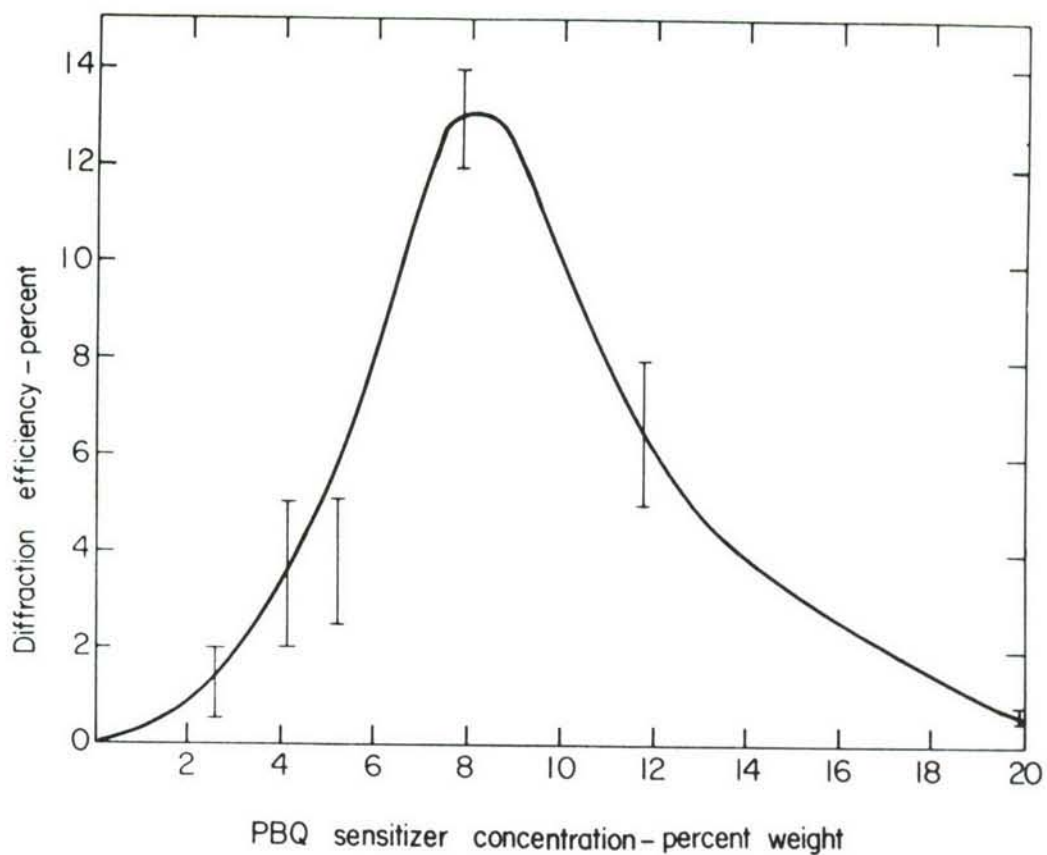
Figure 5.   Diffraction efficiency as a function of sensitizer concentration.
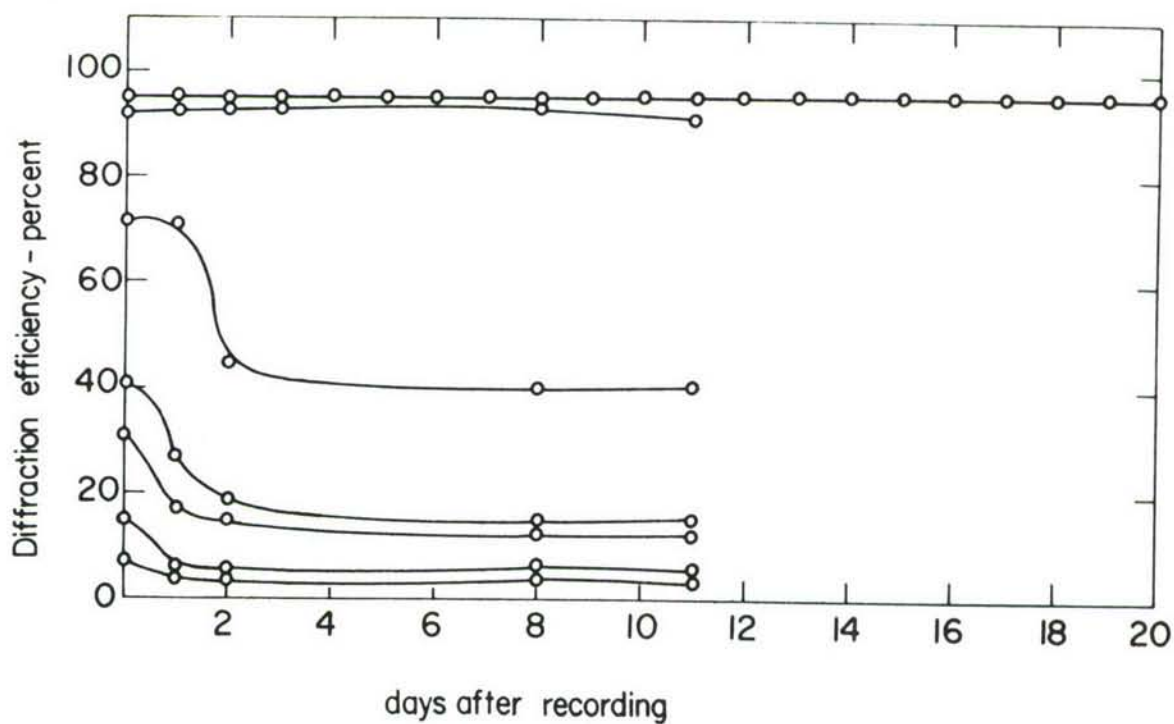
Figure 6.   Temporal stability of recorded holographic gratings.

opaque center. The recording geometry was arranged so that each hologram contained approximately 3×10^6 bits/cm^2 [18]. In readout a photomultiplier scanner was used to measure the powers of the signal to noise. The average signal was determined from a scan across the bright area of the reconstructed image and the average noise determined from a scan across the dark area. We define the ratio of the average signal power to the average noise power to be SNR.

Figure 7 shows the SNR and diffraction efficiency as a function of average exposure for two different sample thicknesses; the reference-to-signal beam ratio was about 4:1, and the average recorded spatial frequency was about 1000 lines/mm. For the 36 microns thick sample the SNR reaches a peak of 200 or 23 dB at a diffraction efficiency of 1.8 percent, whereas for the 107 microns thick sample the SNR reaches a peak of 70 or 18.5 dB at a diffraction efficiency of 5 percent. In both samples the maximum SNR occurs at an average exposure of about 2.2 Joules/cm^2. At the peak diffraction efficiency of 2.3 percent and 8 percent for the 36 microns and 107 microns samples respectively, the SNR decreases somewhat.

2.4. Hologram Formation Mechanism

Holograms are recorded in the photodielectric materials by means of a small variation in their refractive index. This change may be effected in two basic ways: either the density of the material is changed or the molecular polarizability is altered (or some combination of both effects). We conducted a number of experiments that suggest that the primary factor causing a change of refractive index is density increase [19].

In one experiment we recorded simple reflection holograms (two plane wave with $\lambda = 488$ nm) in a photodielectric layer, of 130 microns thickness, and monitored the diffracted intensity during recording with $\lambda = 632.8$ nm. We observed that during recording, the readout beam incidence angle had to be
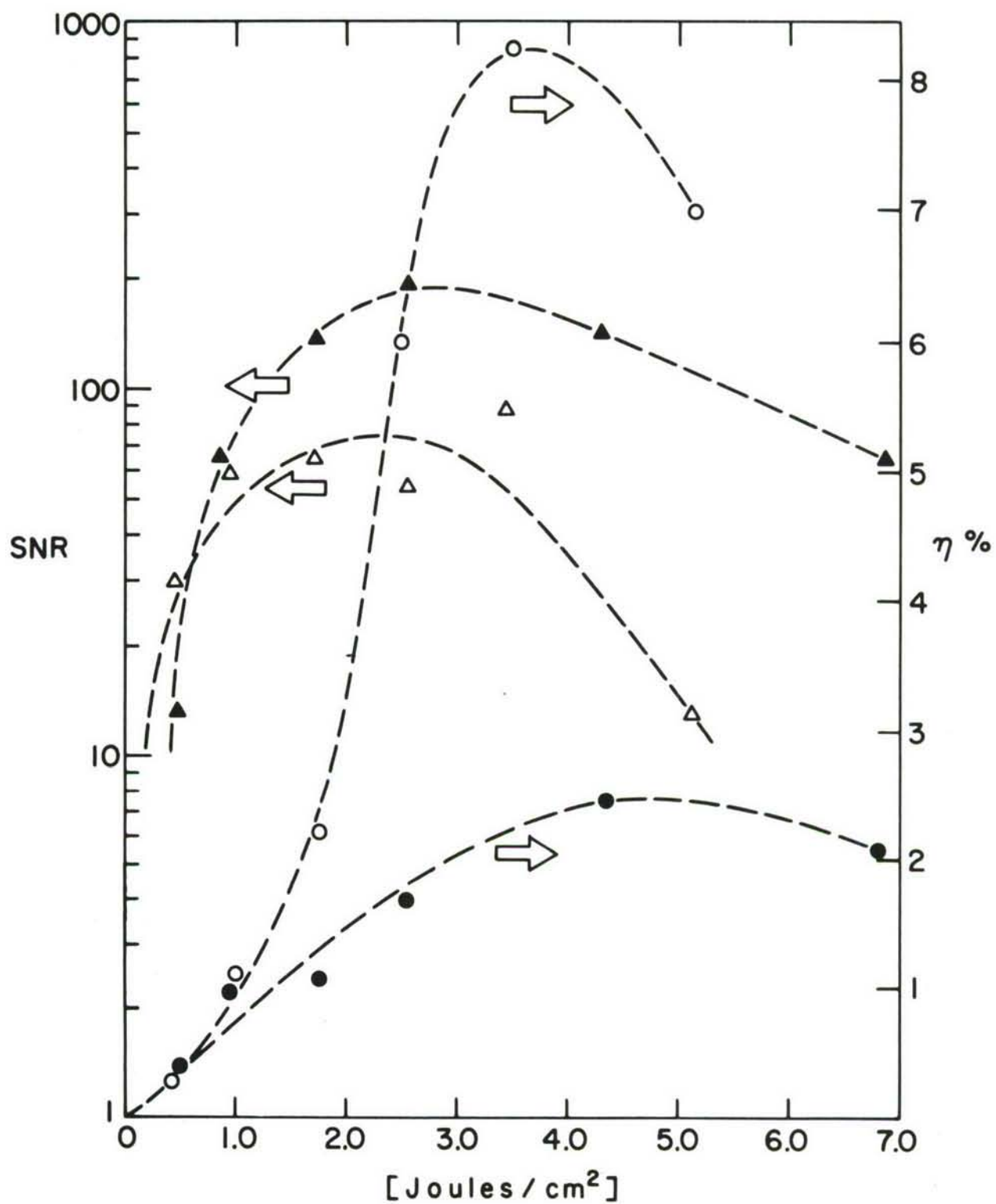
Figure 7. SNR and diffraction efficiences as a function of exposure for different thicknesses.

constantly increased for maximizing the diffracted intensity. We attribute
this behavior to a continual shrinkage of the recording material which reduces
the spacing, d, between the recorded fringe surfaces. As a consequence the
readout angle, θ, must be correspondingly changed to satsify the Bragg
condition, $2d \sin\theta = \lambda$. Note that the effect of this behavior is negligible in
an unslanted transmission hologram, where the boundary conditions are different.

The change in fringe spacing as a function of readout angular change is
obtained from the Bragg relation, to yield

$$\Delta d = - d \cot\theta \, \Delta\theta. \qquad\qquad (2.1)$$

In the experiment the reference and signal beams were oriented at 45° with respect
to the normal of the hologram plane, so that equation (2.1) reduces to $\Delta d = - d\Delta\theta$.
The recorded fringe surfaces are parallel to the front and back surfaces of the
recording medium; thus the relative change $\Delta d/d$ corresponds to a relative
change of the thickness of the medium $\Delta t/t$, where t is the thickness. The
measurements revealed that, as the exposure levels increased, the required
change, $\Delta\theta$, to maximize the diffracted intensity ranged from 0.003 to 0.018
radians, implying a density increase that ranged from 0.3 percent to 1.8
percent.

In another experiment a strip of gold was evaporated on an optically flat
glass plate, which served as a substrate for a 60 microns layer of photodielectric
material. An area of the material was then irradiated with $\lambda = 488nm$ to a certain
high exposure level. This level was such that, if the optical path difference were

due to a change of polarization only, the expected path through the irradiated area would differ by $\frac{\lambda}{2}$ from the non-irradiated area. This was derived from the basic thick transmission hologram diffraction efficiency equation [2o].

$$D.E. = \sin^2 \left[\frac{\pi \Delta n \cdot t}{\lambda \cos\theta}\right] \qquad (2.2)$$

For small incidence angle, θ, and a diffraction efficiency of 1, the predicted value of optical path change should be $\Delta n \cdot t = \lambda/2$. Because of the reflective gold layer, the overall path change becomes λ. When examined microscopically with a Nomarski polarization interferometer, however, the change in optical path turned out to be only $\lambda/4$. Since the overall optical path change is $t\Delta n + n\Delta t$, the discrepancy between the expected and experimental result is due to the term $n\Delta t$. From these results we calculate that the density increase is about 0.6 percent.

In a related interference experiment a stack of ten parallel separate photodielectric plates, each of 130 microns thickness, was placed in one arm of an interferometer, so as to obtain simple interference fringes on some viewing screen. A stack rather than a single 1.3 mm thick plate was used in order to avoid the excessive noise which would be generated in the thick layer for the high exposure level necessary to conveniently detect a change in the material. The stack was irradiated with $\lambda = 488$nm to a near saturation exposure level that would cause a 5 fringe displacement in the observed interference fringe pattern if the refractive index change were only due to molecular polarizability variations. The actual shift however, was 1/2 fringe, indicating a shrinkage of the photodielectric material. The shrinkage is due to a local density increase of about $\frac{\Delta d}{d} = 0.1$ percent. The relatively low density increase measured by this experiment is presumably due to different effective boundary conditions.

The results of the experiments described above provide evidence that index of refraction changes are primarily caused by local increase of density. This is further corroborated by viscosity measurements in solution which demonstrate that the photodielectric materials cross link when irradiated with actinic radiation [21]. The cross linking process can be represented by the following reaction:
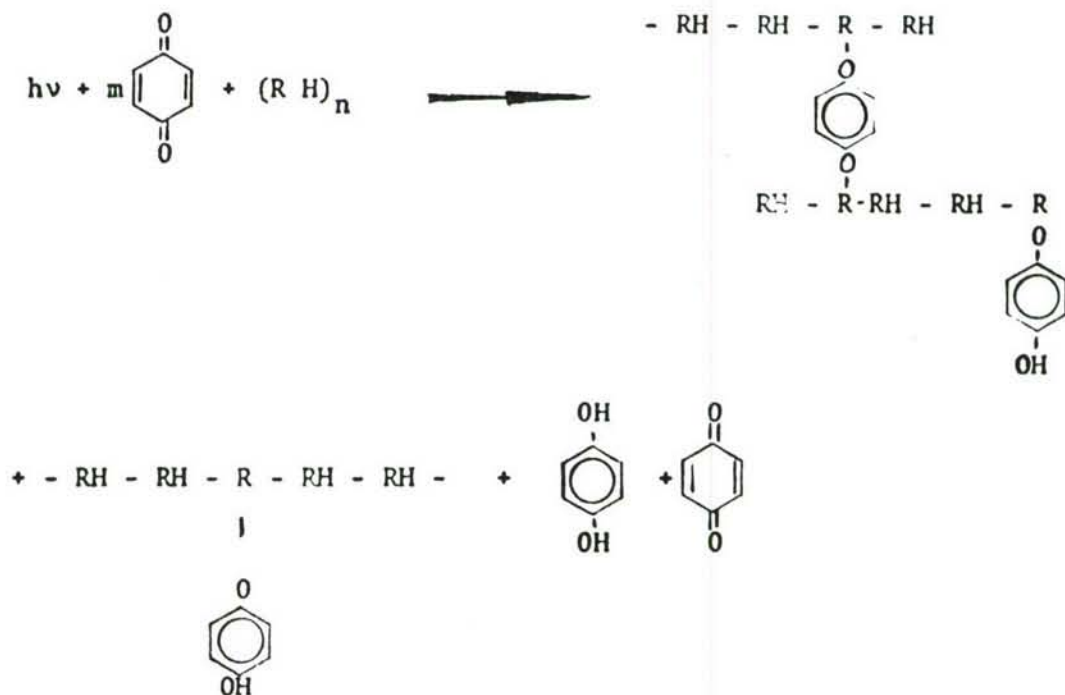
which describes the absorption of actinic radiation and production of free radicals that cross link adjacent polymer chains; the first product in the reaction is due to a crosslinking reaction on the polymer chain with an abstractable hydrogen. The recording mechanism, then, is due to cross links which draw the chains closer together, increasing the density and thus increasing refractive index.

- 19 -

The crosslinking mechanism suggests that the formation of the hologram occurs in the bulk of the material and should be independent of absolute thickness of the device. Indeed, by using equation (2.2) for converting experimental data on diffraction efficiency to index of refraction modulation, Δn, as a function of exposure, we obtain the master curve as shown in Fig. 8.

These results exclude residual monomer photopolymerization as a probable storage mechanism for our material. If this were not the case the residual monomer concentration would have peaked at the center during the preparation of the samples, since the polymerization is initiated at the surfaces; this peaking would obviously be dependent on absolute sample thickness. However, the results of Fig. 8 clearly indicate that the index of refraction modulation is independent of sample thickness.
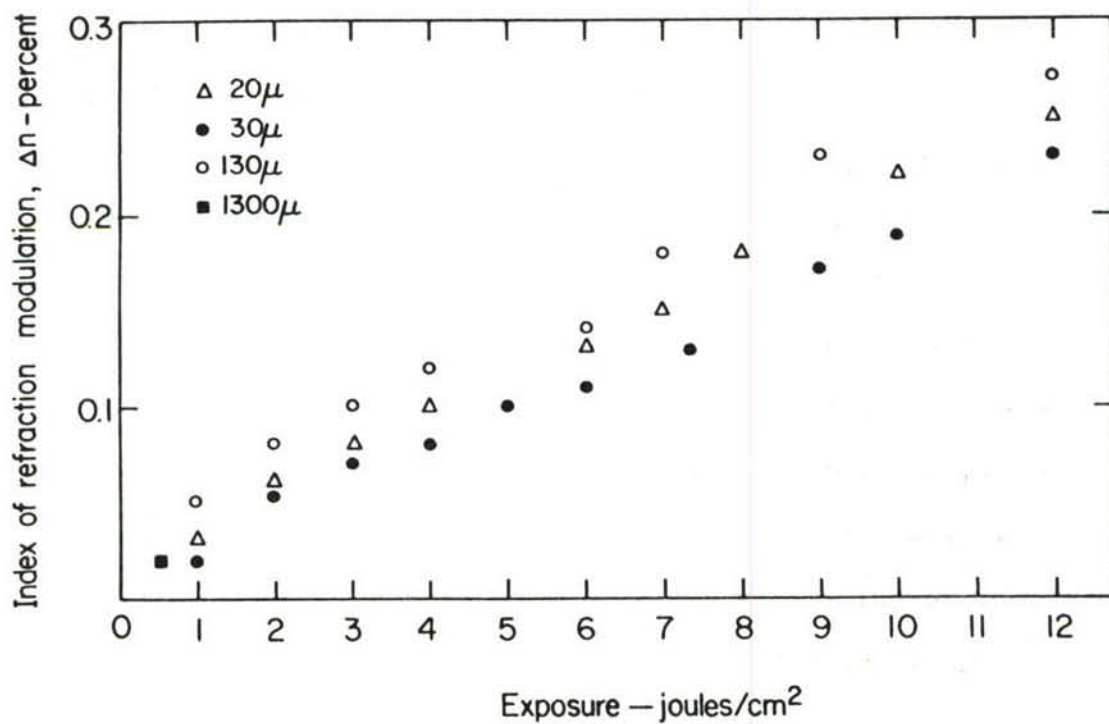
Figure 8.   Index of refraction modulation as a function of exposure for different sample thicknesses.

3. PHOTOCONDUCTOR-THERMOPLASTIC (PC-TP) DEVICES

3.1 General

Photoconductor-thermoplastic (PC-TP) devices are a family of erasable storage materials on which holograms are recorded as surface deformations. The materials are sensitized by a corona discharge to a positive or negative potential, exposed to visible radiation, and developed by heating to the flow temperature. Electrostatic forces produce deformations which are proportional to the light intensity used for exposure, and a stable hologram is formed if the thermoplastic is cooled before surface tension of the plastic layer restores the original smooth surface. The hologram can be erased by heating the thermoplastic layer beyond the softening point. The original smooth surface is restored, and the materials are ready for a new recording cycle.

The salient features of the PC-TP devices which make them most attractive for general holographic applications are: (1) write-read-erase capabilities; (2) in-situ recording, development, and readout; and (3) virtually real-time recording cycle (typically less than 3 seconds). For the holographic non-destructive testing applications, additional attractive features include relatively high exposure sensitivities and panchromatic response.

Although PC-TP devices have been considered for hologram interferometry in the past they suffered from limited recording bandwidth and poor noise characteristics; as a consequence they were confined to recording holograms

of relatively small objects [22,23] . Our investigations of these devices
showed that the bandwidth response may be significantly increased by
controlling the thickness of the device and by proper development techniques.
We shall describe these investigations in some detail and present specific
examples where the devices are incorporated into a HNDT system.

3.2 Principles of Operation

A number of investigators have reported [24-26] on some of the details
of the recording mechanism of photoconductor-thermoplastic devices, so we
confine ourselves to only a brief description of our device configuration
and operation. Refer to Fig.9 that shows a configuration which can be
conveniently prepared. The substrate is an optical grade glass onto which
a thin film of transparent conductor (generally tin oxide or indium oxide)
has been deposited. The conductive layer is used for a ground plane for
the charges deposited on the surface of the thermoplastic. An organic
photoconductor layer is then coated on the transparent conductor and the top
layer consists of a deformable thermoplastic layer.

The hologram is recorded in the PC-TP device as surface deformations
corresponding to the spatial variations of the exposure pattern. The
holographic recording process, which can be described with the aid of
Fig.10, consists of four basic steps:

1. The recording medium is charged (in the dark) to a uniform potential
    by a corona discharge device.
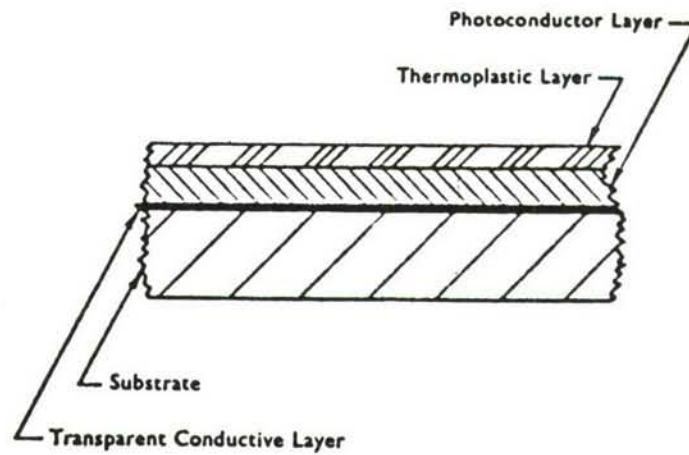
Figure 9 - Photoconductor-thermoplastic recording device configuration.
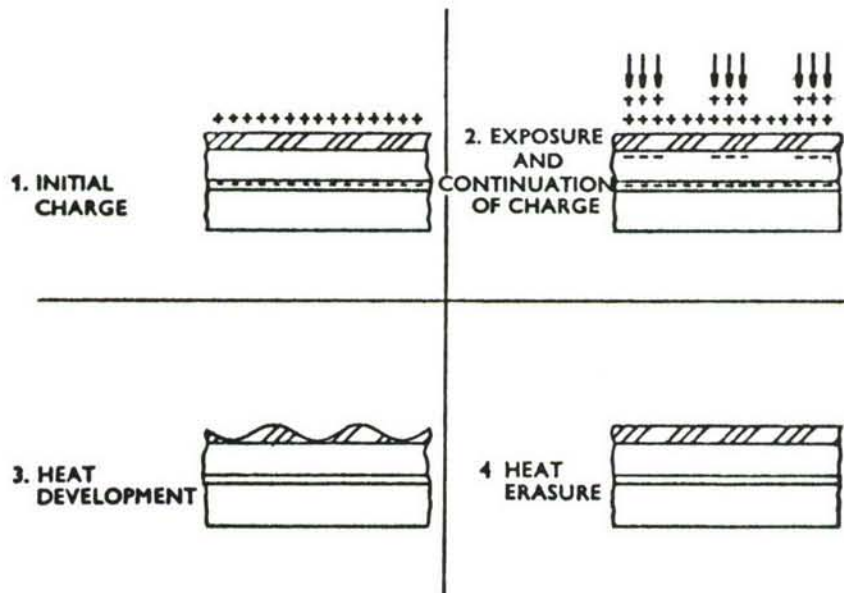
Figure 10. Recording - erasure cycle.

2. The medium is exposed to light, causing a variation of the charge pattern on the photoconductor which corresponds to the variation of the illumination, and is recharged at those areas where the exposure has changed the electrostatic surface potential.

3. The medium is developed by raising its temperature to near the melting point and then rapidly lowering the temperature to the ambient level; surface deformations proportional to the light intensity are produced.

4. The recording is erased by raising the temperature level beyond the melting point to even out the surface deformations.

At present there exists no comprehensive theory which relates the operational parameters such as exposure, charging and heating techniques with the observed holographic response of PC-TP devices. Existing theory is mainly phenomenological, and this is described in a subsequent section.

3.3 Device Fabrication

In the past, one major drawback of PC-TP devices for holographic non-destructive testing was that their recording surface had to be confined to a relatively small area. In particular, PC-TP devices with large areas place severe requirements on materials and fabrication techniques, such as homogeneity of photoconductors and thermoplastic materials, uniformity of recording layers and transparent conductor. For example, any non-uniformity

in either transparent conductor resistivity that is used for development, or in the PC-TP layers, will result in a reduction of the quality of the holographically reconstructed imagery. Furthermore, about 50 W are needed to develop and erase the recorded information in PC-TP devices with areas of $1cm^2$; for larger areas of 100 cm^2, however, about 5kW of power are required, all at switching speeds of the order of 5ms. A major part of our effort, therefore, was devoted to develop fabrication procedures and auxiliary electronic equipment that can handle devices as large as 5cm by 5cm.

A typical device, having an active area of 3cm by 3cm, is shown in Fig.11. The device is cut from a commercially available 3 mm thick glass plate, coated with a conductive, transparent layer of Indium Oxide, having a nominal resistance of 100 Ω/square. To obtain devices with an active recording area of 3 x 3 cm, we begin with a glass plate measuring 5cm by 7cm; after suitable etching, a conductive coating is left only in an area necessary for active recording. The glass plates are then thoroughly cleaned and the thin film electrodes are applied in two steps. First, a thin layer of Cr is evaporated, to assure a good adhesion of the next layer, which may be either one of the four highly conductive metals: Copper, Aluminum, Silver or Gold. These types of electrodes have excellent adhesion, prolonged lifetime, and are capable of withstanding strong electrical currents. The devices are indeed tested by passing through them a current of 5 A prior to the application of the organic films. Those which survive this test (the yield is normally about 90%) are further coated successively with photoconductor and thermoplastic layers.
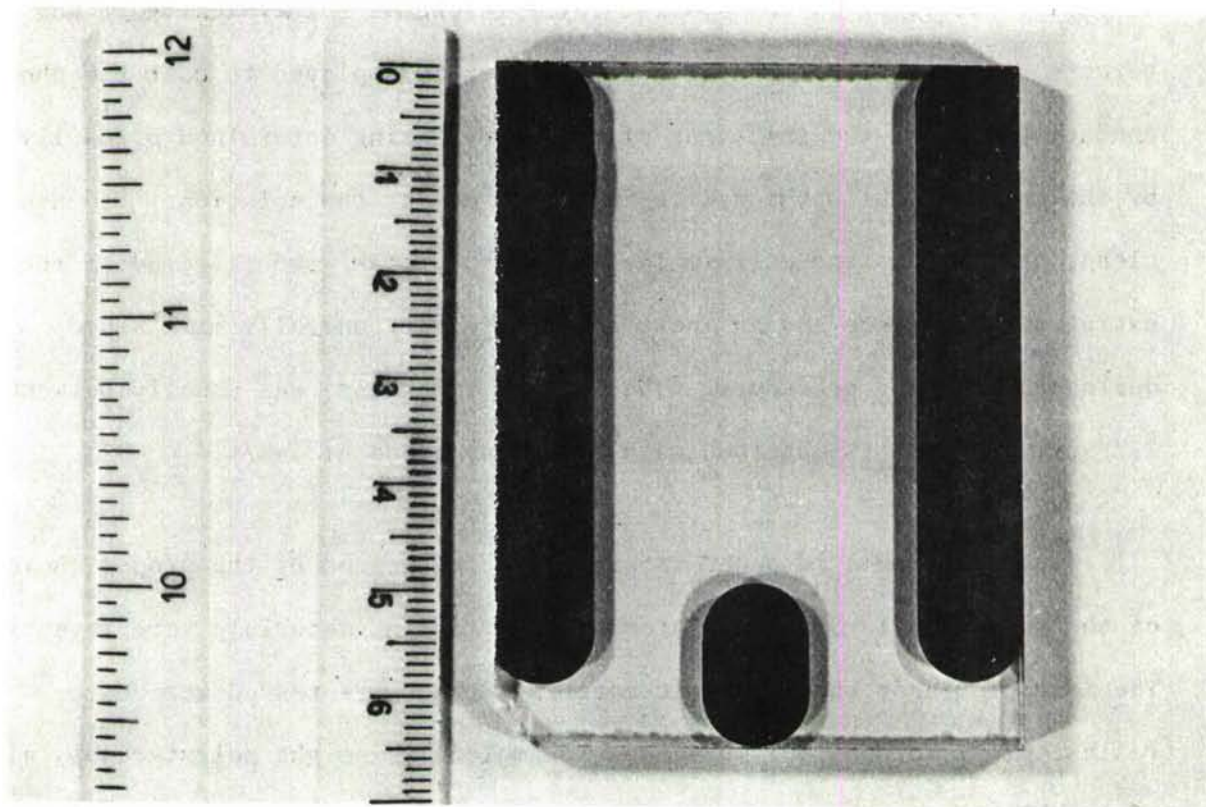
Figure 11. A typical photoconductor-thermoplastic recording device.

The most common photoconductor for our devices was polyvinyl carbazole (PVK) sensitized with trinitrofluorenone (TNF) at the ratio of 10:1. Both materials are dissolved in a mixture of tetrahydrofurane and 1-1-2-trichloroethane at a ratio of 10:1; the concentration of photoconductor in the solvent is varied according to the desired layer thickness but typically it was 7 percent. Dip-coating techniques were generally employed to coat the photoconductive layer; the thickness of the layers being determined primarily by the speed at which the device is pulled out of the solution. To ensure clean, homogeneous and uniform layers all solutions were filtered to remove extraneous substance and an inert atmosphere was generally maintained during the coating procedure. The optimum thickness was usually between 2-2.5μm, and this is obtained with a typical speed of 1mm/s.

The holographic response is primarily influenced by the proper choice of thermoplastic layers, so that several different materials were investigated. The most prominent thermoplastic materials that were tested were ester resins, vinyl-toluene polymers, and low molecular weight polystyrenes, all of which are suitable for HNDT applications. The materials were dissolved in n-Heptane to form a solution which was compatible with the photoconductor. For some materials such as high molecular weight polystrenes, which did not dissolve in n-Heptane, carbon-tetrachloride was substituted for a solvent. However, since the resulting solution tended to interact with the photoconductor layer, an intermediate protective layer of plasma polymerized acrilonitrate was introduced between the photoconductor and thermoplastic layers.

Because it was readily available, inexpensive, and provided good
holographic response, the Foral 105 [27], which is a commercial vinyl-toluene
resin, was the most convenient thermoplastic material. Twenty grams of this
material were dissolved in 100 cc of n-Heptane to obtain a solution which
was then purified. Again dip-coating techniques were employed to obtain a
0.5 microns layer thickness; the pulling speed was 1mm/s. Plasma polymerization
techniques were also investigated particularly with polystyrenes, to form
high quality layers of thermoplastics, but dip coating was less complicated,
and consequently more common. Finally, after coating both the photoconductor
and thermoplastic layers, the devices were baked in a vacuum oven at $60^{o}C$
and at a pressure of 0.2 torr, to remove residual solvent.

A photograph of the overall charging and recording system is shown
in Fig. 12. The system comprises a fixture to hold the PC-TP device, a
corona charging unit, a remote control unit, and an all purpose electronics
console. The console contains the heat development and erasure power unit
and a 7 KV supply for the corona charging. Since it served as a general
investigation tool, the heat development unit had a dual mode capability
for either delivering a multiplicity of heat pulses or a single heat pulse.
The heating parameters could thus be adjusted to suit the requirements
of the different types of devices that were tested.
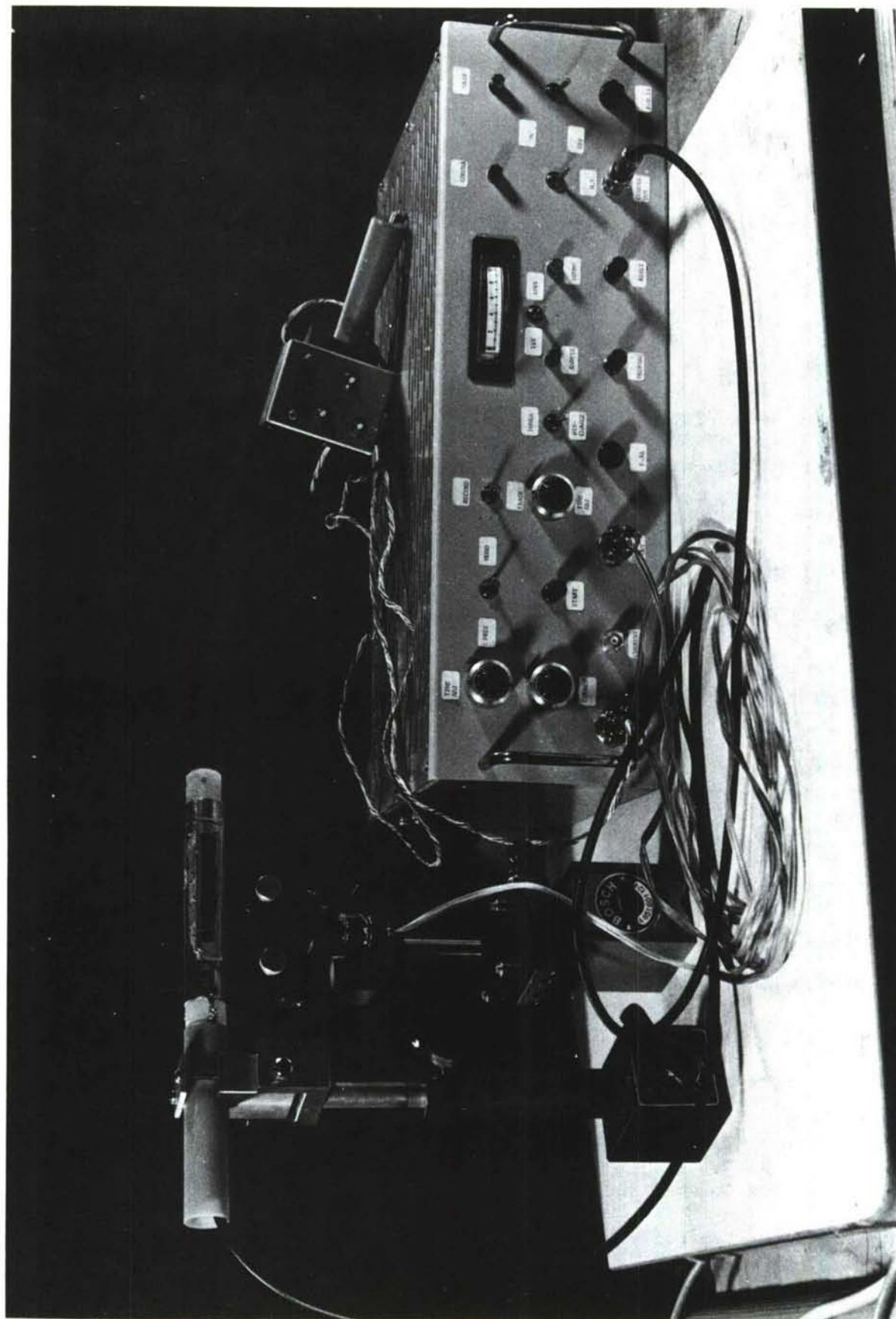
Figure 12. Breadboard model.

For the multiple pulses mode the width of each pulse can be adjusted from 150μsec to 400μsec, and the repetition rate is fixed at 50 cps. In the single pulse model the pulse duration can be adjusted from 2 msec to 40 msec. The heating supply voltage is 300 V in both modes. For erasure the system is switched to "erase" position, and a predetermined longer erasure heat pulse is delivered to the PC-TP device; typically, the duration of the erasure pulse is increased by a factor of three. A safety relay was also included to automatically disconnect the PC-TP device from the development unit shortly after the application of the development or erasure pulses.

The corona unit is mounted on a swivelling fixture. During exposure and development the corona is placed behind the device, facing the thermoplastic layer at a distance of about 3 cm. After development the corona unit is raised to allow readout of the reconstructed imagery.

3.4 Improved Development and Charging Techniques for Better Holographic Response

Although PC-TP devices have been considered for hologram interferometry in the past, they suffered from limited recording bandwidth and thus were confined to recording holograms of relatively small objects. We found that this limited bandwidth response may be due, in part, to improper development heating techniques. For example, in conventional development a single voltage or current pulse of about 100 milliseconds is applied to the transparent conductor to heat the thermoplastic layer beyond its softening temperature, T_g (typically 75°C). The rise in temperature decreases the viscosity of thermoplastic so it deforms in a manner related to the desired holographic interference pattern. Rapid cooling caused by the termination

of the pulse stabilizes the deformation until intentional erasure.

Unfortunately as the viscosity of the thermoplastic layer decreases,
its ionic conductivity increases by the same order of magnitude - generally
3 to 4 - obeying the Nernst-Einstein-Townsend relation,

$$\eta\mu = constant, \tag{3-1}$$

where η is the viscosity of the melt and μ the ionic mobility. The sharp increase
of the conductivity causes partial collapse of the electric field across the
thermoplastic layer, reducing the tension and consequently the deformation;
thus the holographic response is decreased.

Another consequence of the single, relatively long heating pulse is
that the development is inefficient. In particular, as the duration of the
pulse increases,more of the heat propagates into the glass substrate
thereby reducing the developing efficiency. Moreover, as the substrate is
heated the initial ambient temperature of the thermoplastic layer changes
so that a subsequent hologram must be developed with a different heating
pulse duration; otherwise the holographic response will decrease leading
to inconsistent results. An additional difficulty is that the optimal
value of the heating pulse varies as a function of the recorded spatial frequency.
To overcome these difficulties we considered different developing techniques -
some with more success than others.

One attempt was to shape the developing pulse so as to reach a fixed

and constant temperature of the thermoplastic layer. This was achieved with a voltage pulse having an exponentially decreasing amplitude. Unfortunately, no significant improvement in the holographic response was observed.

A different and more successful attempt involved a mode of operation in which the PC-TP device is developed with a series of narrow heat pulses, rather than a single long pulse. In this mode, the duty cycle, the amplitude and the duration of each pulse are chosen so that the thermoplastic layer rapidly reaches a deformation temperature (Tg - glass transition) after each pulse and is cooled before the succeeding pulse is applied. As a result, each pulse causes an incremental deformation which is asymptotically added to earlier deformations. This permits better control of the development so that the holographic diffraction efficiency and bandwidth are improved.

We have experimentally measured the diffraction efficiency and modulation transfer function of the PC-TP devices with this multi-pulses mode of development and the results are shown in Figs. 13 and 14. Figure 13 depicts the diffraction efficiency (diffracted power/incident power) as a function of exposure for simple holographic gratings whose spatial frequencies were 800 lines/mm. The duration of each pulse was 200 microseconds and its amplitude was adjusted to obtain an energy of 0.02 Joules, which for an active area of 1 cm^2 is a small fraction of 1 Joule required to develop a PC-TP device with one pulse. The pulse repetition rate was 100 cps. As shown the diffraction efficiency increases monotonically to a value of 24 percent which is first reached at an exposure level of 1000 ergs.
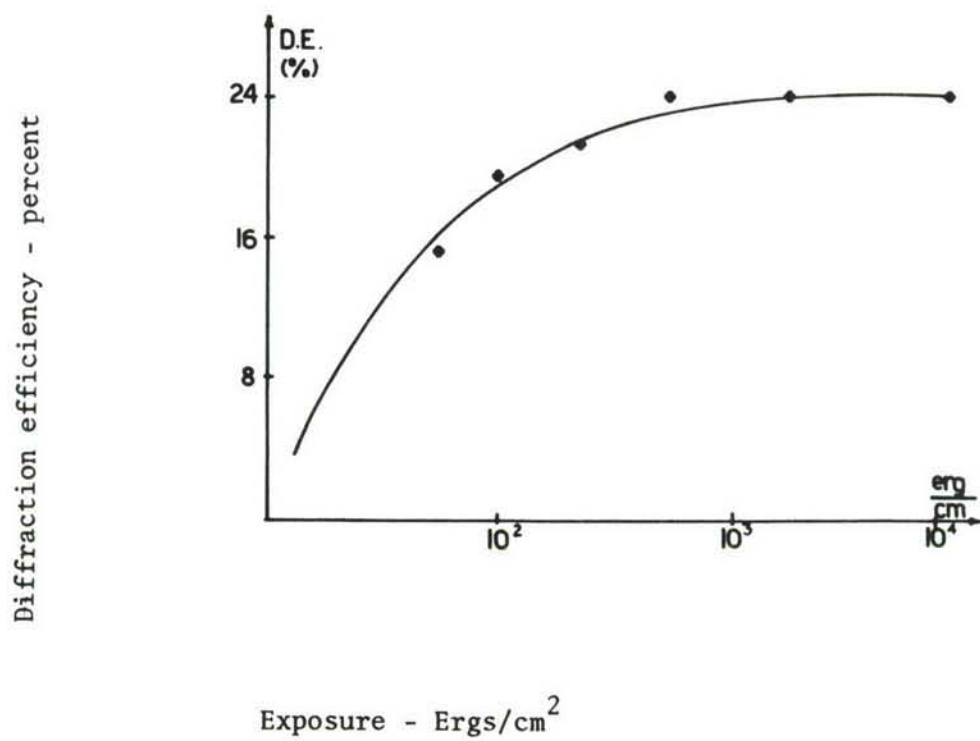
Figure 13 - Diffraction efficiency as a function of
exposure for multi-pulses development.

Spatial frequency - lines/mm
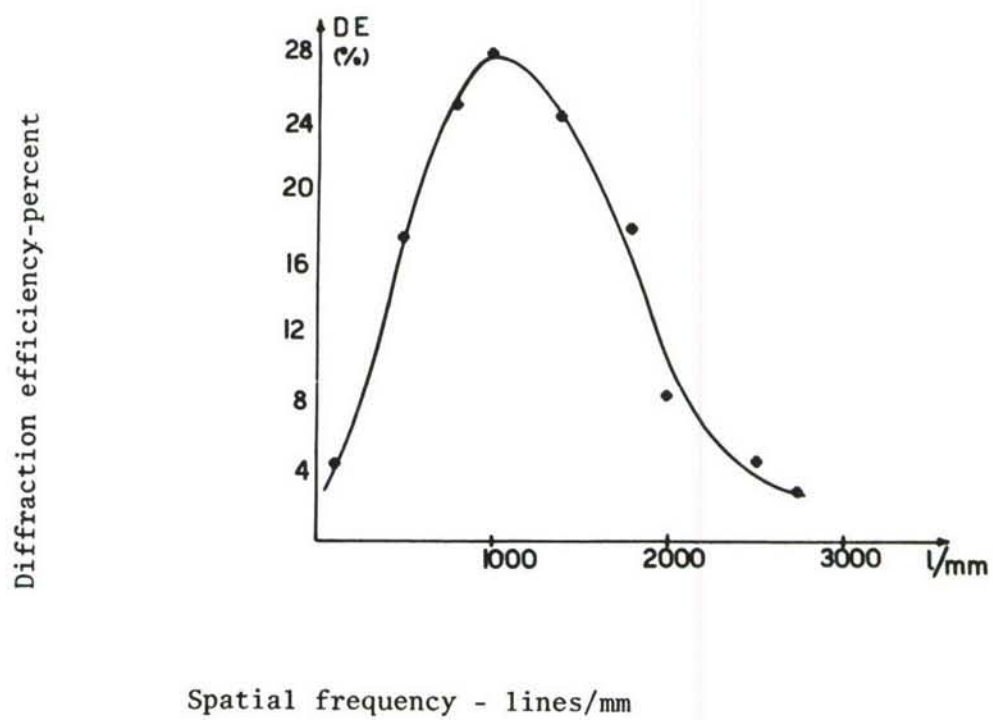
Figure 14. Diffraction efficiency as a function of
spatial frequency for multi-pulses development.

Figure 14 shows the modulation transfer function with the multi-pulses development. The parameters of the sample and the heat pulses were the same as for Fig.13. As shown, the center frequency is 1000 lines/mm and the half power bandwidth is about 1500 lines/mm, which is significantly greater than with conventional single pulse development. We hypothesize that the improvement in bandwidth is due to better utilization of the applied electrostatic force. Specifically, the bandwidth response is usually limited by two restoring forces. The surface tension limits the response of the thermoplastic layer at the higher spatial frequencies whereas the elastic forces within the thermoplastic limit the lower frequencies response [28] . With the multi-pulses development the effect of the restoring forces is reduced by simply increasing the applied electrostatic forces with each successive pulse.

The pulse series development mode gives consistent and reliable response because the pulse series can be readily stopped at any desired instant. Thus, since the response can be readily monitored during the development, it is relatively easy to ensure that the diffraction efficiency, and if so desired the reconstructed imagery, reaches an optimal value before the development is discontinued. Unfortunately, the added charge and heat necessary for this mode of development, have a deleterious effect on the thermoplastic layer; crosslinking is significantly increased,

thereby reducing the signal-to-noise ratio (SNR) and the number of
write-read-erase cycles of the device.

To improve the SNR and number of cycles, we found a suitable com-
promise on the number of development pulses. Specifically, only 3 to
4 pulses are applied for development, each pulse of about 5 msecs duration.
The amplitude of each pulse is dictated by the size of the device and
the interval between pulses is between half to one second. This
modified development mode slightly reduces the diffraction efficiency
and bandwidth response, but the improvements in SNR are significant.
Thus, it is the preferred mode for most HNDT applications.

We also investigated techniques for uniformly charging the PC-TP
devices. For conventional devices with small active recording areas,
the corona charging may be a single stationary unit placed above and
at angle to the recording area so as not to interfere with the
exposing light. In general, this was adequate for obtaining a uniform
charge over a small area. However, for larger recording areas alternative
techniques must be devised.

We considered several schemes, involving both stationary and
moving charging configurations. For the stationary schemes we con-

sidered composite charging units comprised of single units above and below the recording area, or completely surrounding the area. In general the charge uniformity was poor, and in some instances the center of the recording area was not charged at all because of the repulsive forces between the charges arising from different location of the charging unit.

A more successful method with the single pulse development was to move a single corona charging unit across the active recording area. With such a scanning technique, the uniformity of the charge on the thermoplastic layer was sufficiently good to obtain high quality holograms over the largest tested active recording area of 5 cm by 5 cm. For the multi-pulse mode of development, however, it is preferred that the charging unit remain stationary. This was achieved by orienting the PC-TP so that the thermoplastic layer faces away from the exposing light and can be charged with a stationary unit centrally located at a distance of 3 cm from the device. The exposing light for this configuration must, of course, pass through the glass substrate. Such an arrangement was used for most of our HNDT experiments.

3.5 Frost Suppression to Improve Noise Characteristics

An area of continuing concern involves the formation of a random pattern in the thermoplastic layer in addition to the surface deformation which constitutes the holographic recording. This random pattern, known as <u>frost</u>, causes excessive light scattering during readout thereby limiting the signal to noise ratio (29,30). It is generally believed that the frost is formed due to the spontaneous deformation of the charged thermoplastic layer after it reaches a certain melt viscosity. Some dominant characteristics of the frost are: (1) it is dependent on the field applied across the thermoplastic layer with well defined threshold levels; (2) it occurs in the polymer melt; and (3) it has a characteristic scale length so that the random surface perturbations exhibit a predominant spatial frequency bandwidth.

In general the frost formation was considered to be an inherent phenomenon when recording with charged thermoplastic materials, and was attributed to the fluctuations of surface tensions. It was extensively treated theoretically [31-34], but none of the theories, however, are completely satisfying; their predictions do not entirely coincide with the experimental results, and for good reasons, since frost, as we show is not an inherent part of the recording process. During the course of the contract we conducted a series of experiments which suggest that the frost formation is primarily due to spinodal decomposition processes [35] . This decomposition may occur in multicomponent systems, such as polydispersed [34] and plasticized [29,31,33,36] polymers.

The probability of spinodal decomposition is even greater with the PC-TP devices since the thermoplastic layer is very thin, having low thermal capacity. In the molten state, when a high electric field of about 10^6 volts/cm is applied, spinodal decomposition may be induced [37,38]; the frost-like pattern resulting from this decomposition is frozen into the thin thermoplastic layer due to rapid temperature quenching upon cooling.

It is well established experimentally that the spinodal decomposition process in polymer-solvent systems as well as in polymer-polymer systems leads to preferential growth of domains exhibiting certain characteristic scale lengths [39]. In fact Cahn showed that during spinodal decomposition, concentration fluctuations with wave numbers β smaller than a critical number β_c, increase in amplitude with time whereas fluctuations with β greater than β_c decreases in amplitude and finally disappear [40].

For light scattered from a system which has undergone spinodal decomposition, the scattering can be described as a reflection of the incident beam on planes perpendicular to the $\vec{\beta}$ vector with spacing $\Lambda = 2\pi(\vec{\beta} \cdot \vec{\beta})^{-1/2}$ for which the Bragg reflection condition $2\Lambda \sin \theta/2 = \lambda$ is obeyed [41]. This reflection manifests itself in a far field annular scattering pattern, which is characteristic of frosted PC-TP devices [29].

The above consideration resolves an old dilema in the domain of the thermoplastic recording materials - the so-called "factor of two rule".

This rule, which follows from an oversimplified interpretation of Budd's work [32] states that the maximum response of the thermoplastic layer as a function of spatial frequency (ν) is achieved for $(\nu_{max} \times d)^{-1}=2$, where d is the thickness of the thermoplastic layer. However, as found by a number of investigators the experimental results are inconsistent with this rule [42,43]. A more likely explanation is that the frost formation process is primarily due to spinodal decomposition; then, for a given thickness of the thermoplastic layer under a constant value of the electric field, a whole range of ν_{max} values might be observed. This is due to the time dependent character of the spinodal decomposition process. Quenching the process at various time stages would result in band limited light scattering patterns centered around a different value of the spatial frequency.

The assumption that frost formation is mainly due to spinodal decomposition suggests that a truly monocomponent thermoplastic layer, for which spinodal decomposition cannot occur, would not develop frost. Such a choice would thereby lead to PC-TP devices with improved signal-to-noise characteristics and high diffraction efficiencies. On the other hand, if the thermoplastic layer contains a solvent or if it is comprised of a polymer with high enough polydispersivity in its molecular weight distribution, frost will undoubtedly form.

To verify the above contentions we selected polystyrene of well defined molecular weight as the monocomponent thermoplastics (see Table I). These were dissolved in spectroscopic grade carbontetrachloride, and by employing dip

coating techniques, a thin thermoplastic layer of about 0.5 micron was obtained. The solvent was subsequently evaporated under vacuum at 70°C for 24 hours. We also tested a mixture of two monocomponent polystyrenes (2220MW with 9168MW), polydispersed styrene of 20000MW, and commercially available Foral 105 [27,45].

TABLE   I

Polystyrene Materials [44]

M_n	M_w/M_n	M_v (Viscosity Average)
900+5%	<1.10	-
2220+5%	<1.06	2400+5%
3100+5%	<1.10	3600+3%
9168+5%	<1.06	9177+5%

To evaluate PC-TP devices with the different thermoplastic layers we measured their diffraction efficiencies and signal-to-noise ratios under the same holographic recording geometries, exposure levels, and development conditions; the average recorded spatial frequency was about 800 1/mm, the exposure was 70 microjoules/cm^2, and the development heat pulse was 5 msecs.

To determine diffraction efficiency, we recorded simple interference gratings by using plane waves for both reference and signal beams. In readout we measured the diffracted laser beam power, Pd, and the incident beam power, Pi; the diffraction efficiency, Pd/Pi, was then calculated from these measured values. The effect of frost on the simple holographic gratings is illustrated in the photographs of Fig. 15. The magnified portion of the holographic grating recorded in a multi-component thermoplastic (Foral 105) is shown in Figure 15(a), where the frost is obviously in evidence. Whereas, Figure 15(b) shows that when the grating was recorded in a monocomponent thermoplastic, such as polystyrene with molecular weight of 900, no frost was formed.

To measure the signal-to-average noise ratio, SNR, we recorded Fresnel holograms of a diffusely illuminated data mask consisting of a square with an opaque center. The recording geometry was arranged to obtain an information packing density of about 3×10^6 bits/cm^2 [18]. In readout a photomultiplier scanned the reconstructed real image, and the SNR was determined from the ratio of the intensity in the bright region to that in the dark center.

Some typical results are summarized in Table II, which gives the diffraction efficiencies and signal-to-average noise for the early recordings as a function of different thermoplastic materials. As shown the SNR for the monocomponent polystyrenes is significantly better than polydispersed and multicomponent materials, while the diffraction efficiency is relatively constant.
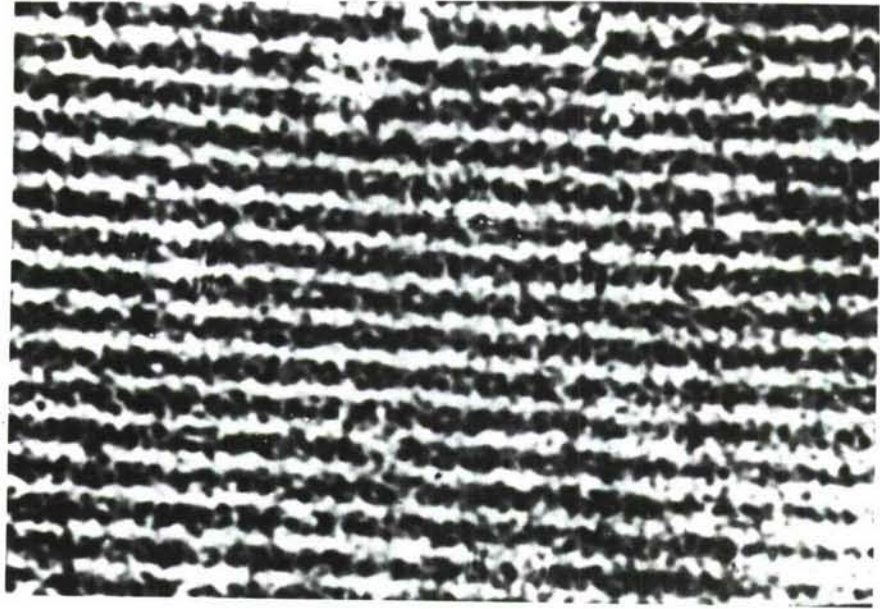
(a)
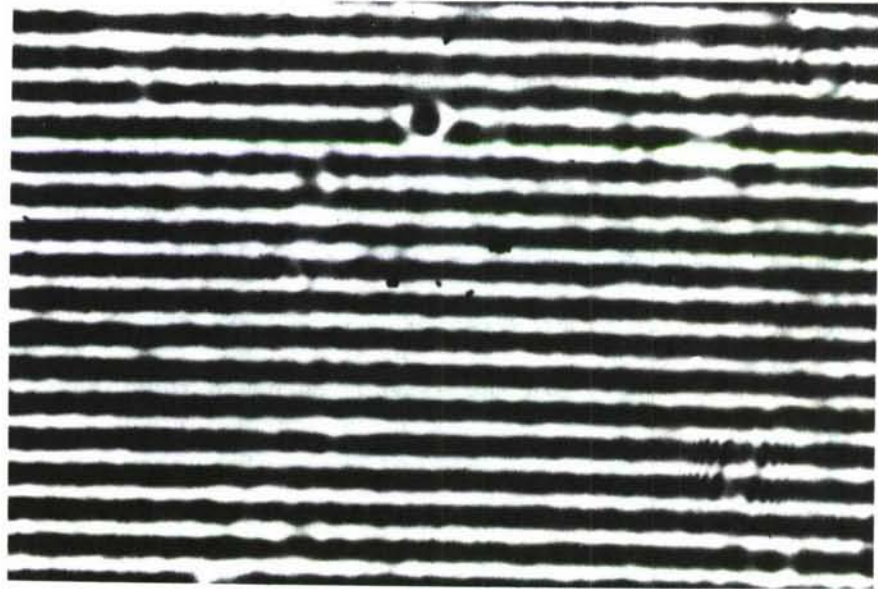
(b)

Figure 15.   Magnified portion of a simple holographic grating;
             actual grating period: 1.25µm. (a) Recorded in
             multicomponent thermoplastic - Foral 105.
             (b) Recorded in monocomponent thermoplastic -
             PS-900 MW.

T A B L E   II

Experimental   Results

	"PS 20000" Polydispersed	"Foral 105"	"PS 9000"	"PS 2000"
SNR	25	15	175	200
DE	7%	20%	12%	15%

The effect of molecular weight distribution of a two component thermoplastic material ("PS-2200MW" and "PS-9000MW"), is shown in Fig. 16. At the two extremes where the material is essentially monocomponent either PS-2200MW at 0 or PS-9000MW at 1.0, the SNR is relatively high as expected. However, as the two materials mix, the SNR decreases, and for these materials it appears that the lowest value of SNR is reached in the vicinity of an equal mixture.

We also measured the SNR of PC-TP devices with monocomponent thermoplastics as a function of the number of record/erase cycles, and the results for the monocomponent "PS-9000MW" are shown in Fig. 17.   The SNR decreases rapidly from about 175 to 50 and after about 40 cycles it reaches a level of about 20 - comparable to multicomponent thermoplastics. The diffraction efficiercies were maintained approximately constant at about 12 percent. Frost became noticable after about 10 cycles, and its intensity continued to increase toward a constant level after 40 cycles. We attribute
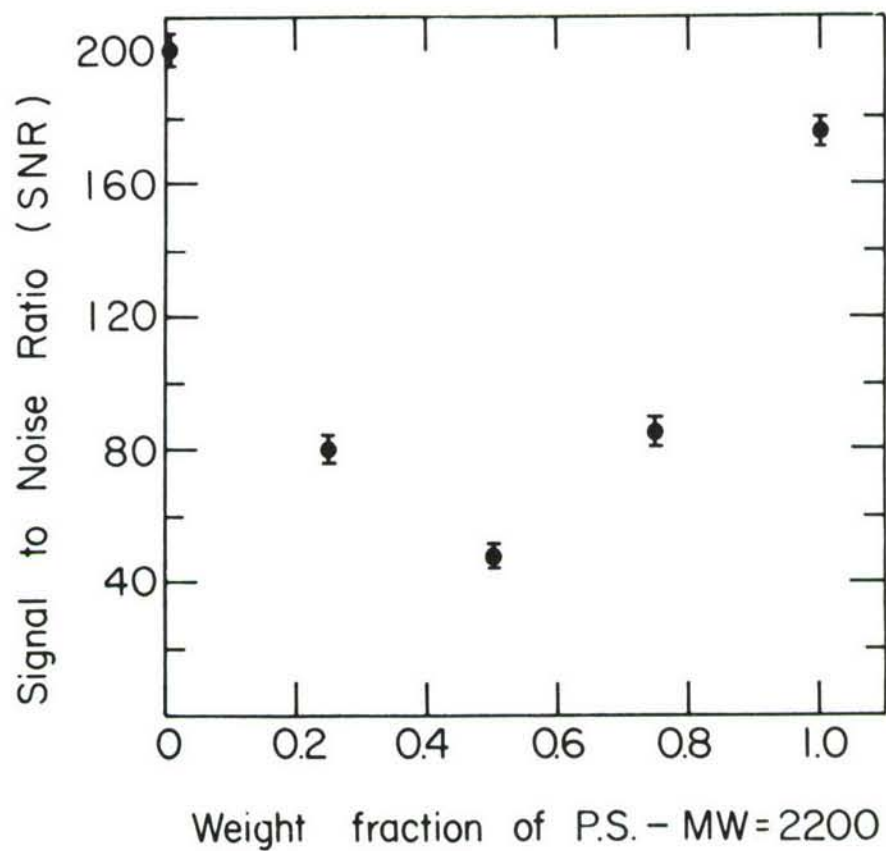
Figure 16. Signal-to-average noise ratio (SNR) as a function of
molecular weight distribution for a two component
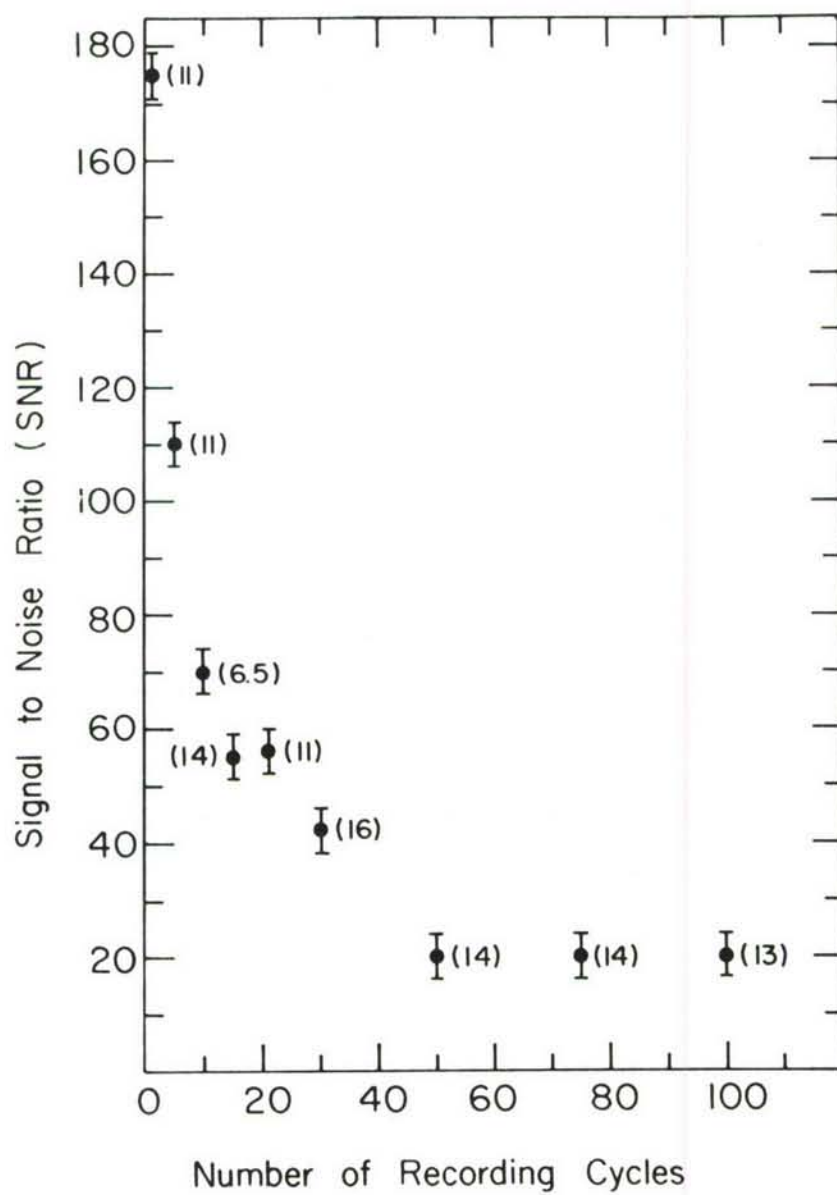thermoplastic: PS-2200 MW and PS-900 MW.

Figure 17. SNR as a function of number of recording
cycles for a monocomponent thermoplastic-
PS 9000 MW. Numbers in parentheses indicate
diffraction efficiency.

This SNR deterioration to the combined action of heat and corona charging in air which probably cause scission of the monocomponent polystyrene molecules to yield a polydispersed distribution which is susceptible to spinodal decomposition.

To summarize, we attribute the frost formation in PC-TP devices to spinodal decomposition. This decomposition may be avoided by using certain monocomponent thermoplastic materials, so that the frost formation is significantly suppressed. Indeed, our tests with monocomponent polystyrenes demonstrate that the frost is essentially eliminated during the first ten record/erase cycles, thereby obtaining excellent signal-to-noise characteristics [46].

In spite of its advantages, the frost-free devices are not so convenient for many HNDT applications. One problem arises, ironically, because of the absence of frost making it difficult to monitor the development of the hologram (i.e. determine the exact number of heat pulses necessary for optimum development). Although it is possible to monitor the diffracted light power, it is not as convenient. Another problem is their relatively lower bandwidth response which we have not, so far, resolved. Thus, although the frost free devices are potentially better for many holographic applications, they are not yet as useful for HNDT.

3.6   Experimental Procedure and Results

To evaluate the PC-TP devices we incorporated them into a conventional
holographic non-destructive testing set-up for identifying disbonds in
multilayered honeycomb structures [46] .   The holographic recording and readout
arrangements necessary for double exposure, time average, and real time
interferometry were employed; the illumination source was an argon ion CW laser
emitting green light of 514.5 nm wavelenth.

For the experimental examples that will be shown both vacuum and
vibration stressings were used for the tests.   The vacuum stressing was applied
either by attaching a transparent plexiglass chamber to the flat surface
of the tested honeycomb panel or by inserting the panel into a large transparent
vacuum chambers so the panel was iluminated and viewed through the chamber.
For the vibration stressing the test samples were excited by a piezoelectric
transducer, driven by an oscillator through a power amplifier.   The appropriate
resonant frequencies, at which a maximum number of disbonds were excited,
were first recorded using either speckle or real time inspection, and then
time average recordings were made.

Some examples of the results that were obtained with the various holographic
and stressing techniques are given in Figs.18 through 21.   Figure 18 shows
the fringes produced by double exposure holographic interferometry on one
epoxy-bonded aluminum-to aluminum core test panel subjected to vacuum stress;
each of the three photographs depicts the reconstructed imagery from separate
holograms, each recorded with a different stress differential.
The overall area of the panel was 15cm by 20cm, and a disbond region was
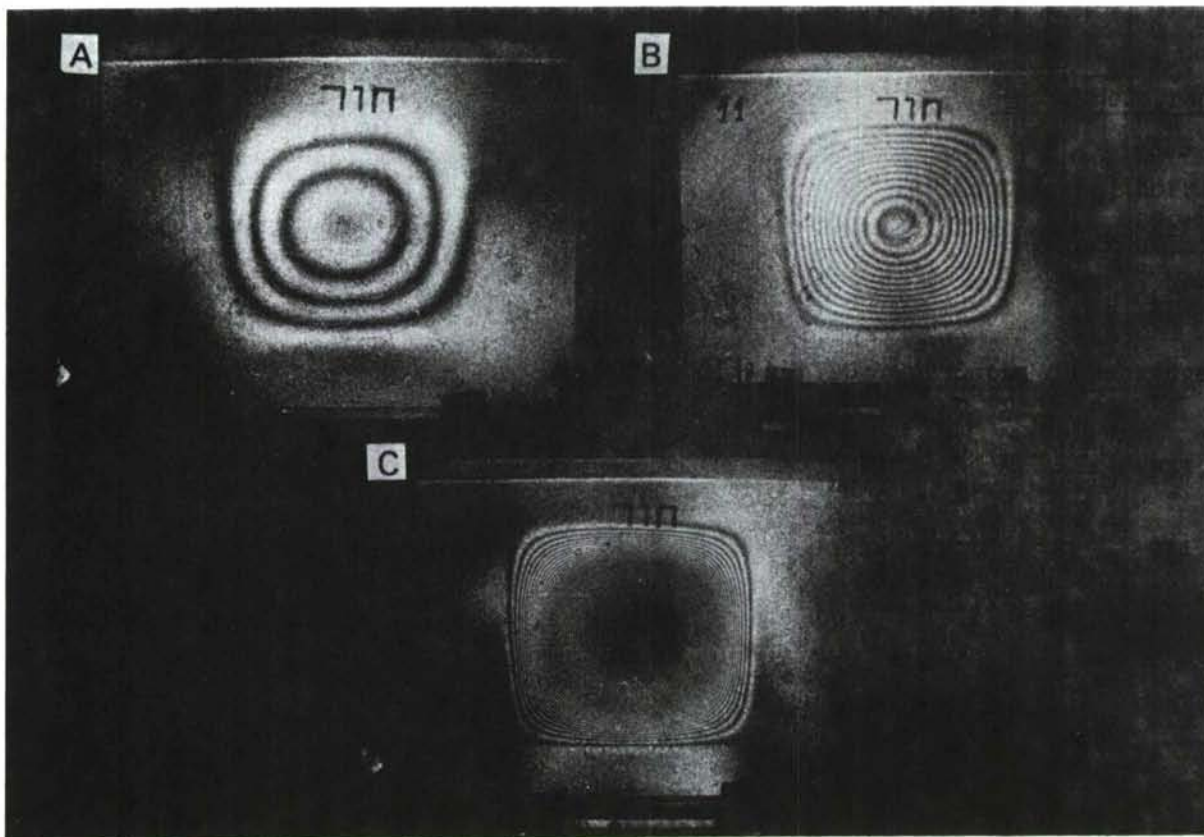introduced by cutting an aperture in the bonding material.   This large

Figure 18. Double-exposure HNDT of 15x20 cm aluminum-to-aluminum bonded honeycomb panel, which contains a deliberate disbond at the center. Stressing by vacuum, the 3 holograms were recorded at various pressure differentials.

disbond area in the center, having approximately a square shape, is clearly evident in the experimental results.

To illustrate the wide bandwidth capabilities of the PC-TP devices, we recorded holograms of a relatively large, epoxy-bonded aluminum-to-aluminum core test panel. The recording geometry and size of the panel, 20cm by 30cm, were such that the effective recorded bandwidth was about 1000 lines/mm; the center frequency was approximately 1500 lines/mm. Two disbonds were purposely introduced by inserting mylar discs between the skin of the panel and the bonding layer. Two examples of reconstructed imagery from double-exposure holograms, made by changing the pressure difference under vacuum stressing conditions, are shown in Fig.19. The two photographs show the test panel with superimposed fringes, at the location of the disbonds.

Similar test panels were also investigated by time average holographic technique. Figure 20 shows the reconstructed images from four holograms, each recorded with a different drive frequency; the test panel was the same as that used in Fig.18. As shown, only the disbond area is excited while the rest of the panel remains stationary.

One difficulty with vibration stressing of honeycomb panels is to determine the proper resonant frequency which will excite the disbond areas only. This necessitates some means for concommitant observation of the interference patterns. Consequently, our holographic set-up included two devices for holographically recording the same test panel. One device served to monitor in real-time   the interference pattern as the vibrating transducer frequencey was varied. At selected frequencies the other device recorded time-average holograms having excellent fringe visibility.
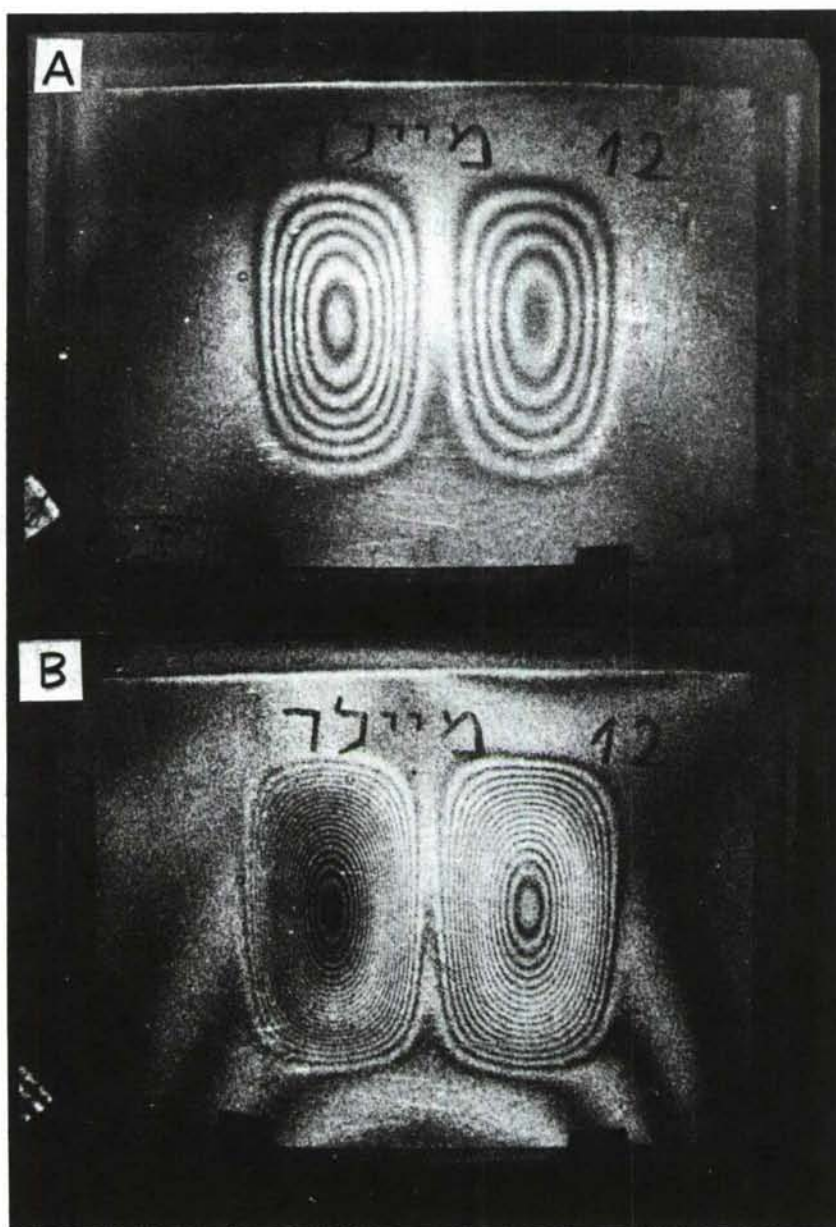
Figure 19. Double-exposure HNDT of a honeycomb panel, with two disbonds at the center.
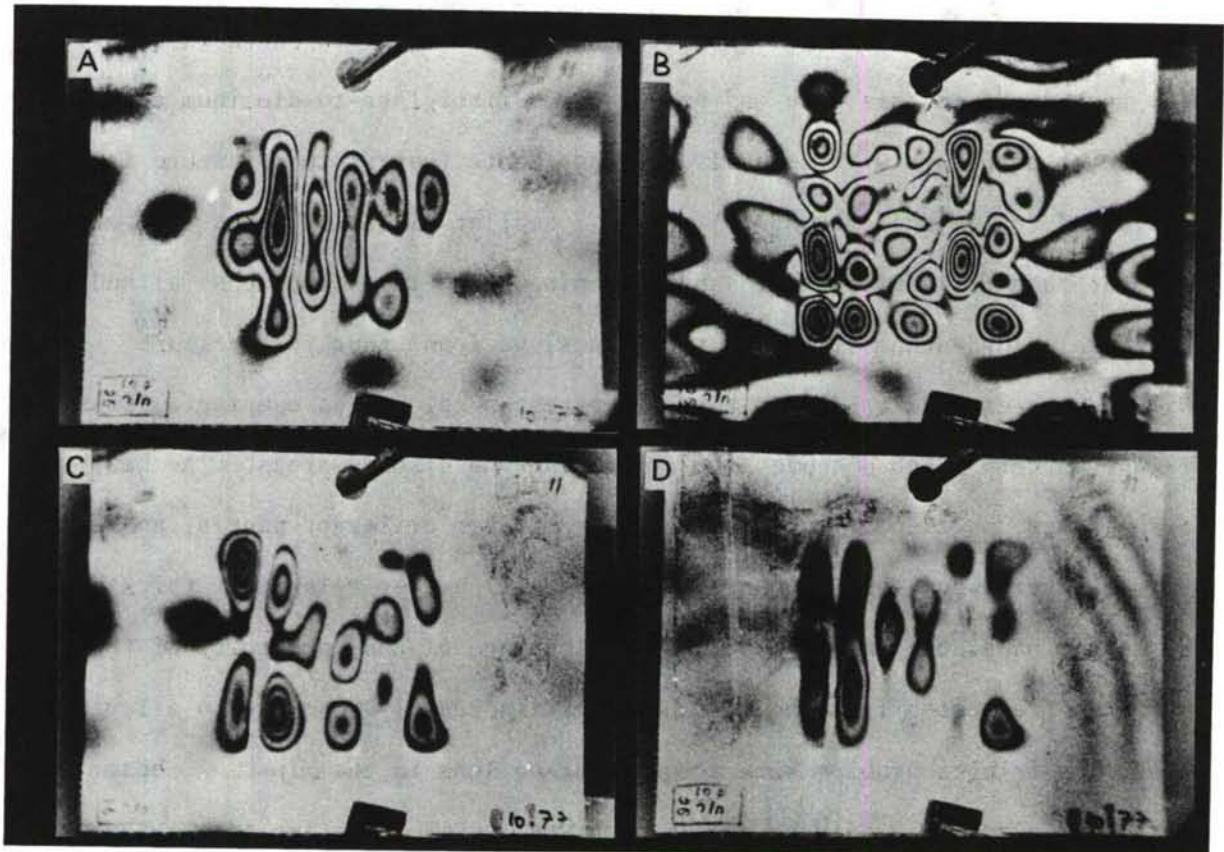
Figure 20. Time-average HNDT of same panel as in Figure 18. Stressing by a piezoelectric shaker. The 4 holograms were recorded at different frequencies.

Representative examples of real-time interferences, made by changing the pressure difference, under vacuum stressing conditions are shown in Fig.21. The test panel in this case was epoxy-bonded fiberglass-to-aluminum core honeycomb structure with several disbonds. Note that as the pressure is increased, as in photographs (c) and (d), smaller disbonds become more clearly evident than for the lower pressure examples shown in photographs (a) and (b). When employing vacuum stressing techniques, we found that for pressure differences exceeding 50 torr the entire test panel bulges causing a "bias" fringe pattern which obscures the fringes at the disbond areas. The bias fringes were particularly excessive with thinner or larger panels, and would become severe when testing honeycomb structures having relatively thick skins. Since the panel bulging causes an overall change of the sphericity of the wavefront reflected from the test panel, it is readily possible to alleviate this bias fringes problem with a compensating lens in the object beam. This, of course, can only be done conveniently with real-time interferometry techniques.
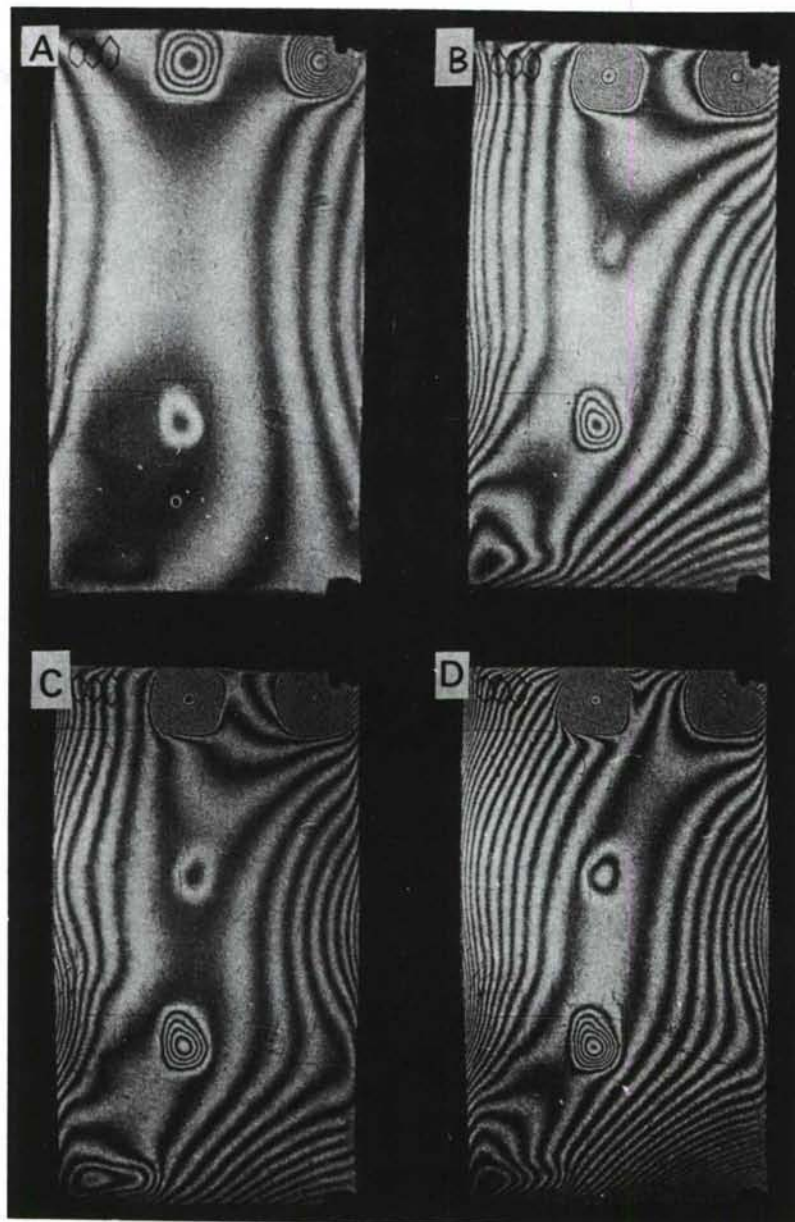
Figure 21. Real-time HNDT of 15x30 cm fiberglass-on-aluminum honeycomb panel. Stressing by vacuum, the photographs were all taken consecutively through the same PC-TP hologram, at various pressure differentials.

4. CONCLUSIONS

A novel photodielectric polymer system for recording in-situ, self-developing, high efficiency volume holograms was described. Laser radiation at short wavelengths (below $\lambda = 520$ nm) produce refractive index variations, thus recording phase holograms. The index change was found to result from localized density increases arising from photo induced cross linking. The salient features of the recording materials are ease of preparation; superior chemical and dimensional stability; in-situ self developing capabilities, diffraction efficiencies in excess of 90 percent; resolution greater than 2000 lines/mm; and excellent noise characteristics. However, because of shortcomings such as low exposure sensitivity and orthochromatic sensitivity, the photodielectric materials are not so attractive for HNDT, except possibly where the objects to be tested are small so the light levels can be sufficiently high.

More attractive holographic storage media for HNDT are the photoconductor-thermoplastic (PC-TP) devices. These are a family of erasable recording materials on which holograms are recorded as surface deformation. The salient features of the PC-TP devices are (1) write-read-erase capabilities; (2) in-situ recording, development, and readout; (3) virtually real-time recording cycle (typically less than 3 seconds); (4) high exposure sensitivities; and (5) panchromatic response. During the course of the program we have developed techniques and means for operating the PC-TP devices more reliably and for improving the spatial bandwidth to over 1800 ℓ/mm.

Furthermore, the deleterious frost formation was investigated, and means

for suppressing the frost were determined, thereby improving the noise

characteristics. These results, together with the high exposure

sensitivities (50 ergs/cm^2), and the improvement in sample fabrication,

have led to an operable device which was incorporated and tested in a

modest holographic non-destructive system. Because of premature termination

of the program, the development of an overall practical camera was not

concluded and tested in other HNDT systems. Since the feasibility was

adequately demonstrated, we expect that an additional year is necessary

to finalize the camera development.

REFERENCES

1. E.R. Robertson and J.M. Harvey (editors), The Engineering Uses of Holography, Cambridge University Press, Oxford, England, 1970.

2. R.S. Sharpe (editor), Research Techniques in Nondestructive Testing, Vol. II, Ch. 7, Academic Press, London and New-York, 1973.

3. R.K. Erf (editor), Holographic Nondestructive Testing, Academic Press, New-York and London, 1974.

4. E.R. Robertson (editor), The Engineering Uses of Coherent Optics, Cambridge University Press, Oxford, England, 1976.

5. W.J. Tomlinson, I.P. Kaminow, E.A. Chandross, R.L. Fork and W.T. Silfvast, Appl. Phys. Lett. $\underline{16}$, 486 (1970).

6. J.M. Moran and I.P. Kaminow, Appl. Opt. $\underline{12}$, 1964 (1973).

7. M.J. Bowden, E.A. Chandross, and I.P. Kaminow, Appl. Opt. $\underline{13}$, 112 (1974).

8. F.P. Laming, Society of Plastics Engrs. Tech. Meeting, Oct. 1970; and Pol. Eng. Sci. 11, 421 (1972).

9. R.G. Zech, J. Opt. Soc. Am. $\underline{62}$, 1396A (1972).

10. A. Bloom, R.A. Bartolini, and D.L. Ross, Appl. Phys. Lett. $\underline{24}$, 612 (1974).

11. J.A. Jenney, J. Opt. Soc. Am. $\underline{60}$, 1155 (1970).

12. W.S. Colburn and K.A. Haines, Appl. Opt. $\underline{10}$, 1636 (1971).

13. B.L. Booth, Appl. Opt. $\underline{14}$, 593 (1975).

14. W.J. Tomlinson, E.A. Chandross, H.P. Weber, and G.D. Aumiller, Appl. Opt. $\underline{15}$, 534 (1976).

15. F. Leonard, R.R. Kalkarni, G. Brandes, J. Nelson and J.J. Cameron, J. Appl. Pol. Sci. $\underline{10}$, 259 (1969).

16. H.W. Coover, Jr., F.B. Joynes, N.H. Shearer, Jr., and T.H. Wicker, Jr., SPE Journal, 413 (1959).

17. Z. Malcom Bruce, The Chemistry of Quinoid Compounds, Part 1, Chapter 9, J. Wiley and Sons, (1974).

18. W.H. Lee and M.O. Green, J. Opt. Soc. Am. $\underline{61}$, 402 (1971).

19. S. Reich, A.A. Friesem and Z. Rav-Noy in Applications of Holography and Optical Data Processing, Pergamon Press, Oxford, England, 1977.

References (cont.)

20. H. Kogelnik, Bell. Syst. Tech. J. 48, 2909 (1969).

21. Y.L. Freilich, M. Levy, and S. Reich, J. of Polymer Sci., 15, 1811 (1977).

22. J.C. Bellamy, D.B. Ostrowsky, M. Poindron, and E. Spitz, Appl. Opt. 10, 1458 (1971).

23. V.N. Thinh and S. Tanaka, Japan J. Appl. Phys. 12, 1954 (1973).

24. J.C. Urbach and R.W. Meier, Appl. Opt. 5, 666 (1966).

25. L.H. Lin and M.L. Beauchamp, Appl. Opt. 9, 2088 (1970).

26. W.S. Colburn and E.N. Tompkins, Appl. Opt. 13, 2934 (1974).

27. From - Hercules Inc., Wilmington, Delaware.

28. D.Kermisch, Image Formation Mechanism in the γ-Ruticon, Technical Report, Xerox Webster, N.Y.

29. T.C. Lee, Appl. Opt. 13, 888 (1974).

30. A.A. Friesem, Z. Rav-Noy and K. Stadler, in Advances Signal Processing Technology, p. 249 (Journees d'Electronique EPF Lausanne 1975).

31. P.J. Cressman, J. Appl. Phys. 34, 2327 (1963).

32. H.F. Budd, J. Appl. Phys. 36, 1613 (1965).

33. U. Killat, J. Appl. Phys. 46, 5169 (1975).

34. D.L. Matthies, W.C. Johnson and M.A. Lampert, J. Appl. Phys. 46, 2956 (1975).

35. S. Reich, Z. Rav-Noy and A.A. Friesem, Appl. Phys. Letters 31, 654 (1977).

36. R.L. Gravel, Appl. Optics 14, 2054 (1975).

37. R.C. deVekay and A.J. Majumdar, Nature 225, 172 (1970).

38. R.W. Hopper and D.R. Uhlmann, Phys. & Chem. of Glasses 14, 37 (1973).

39. L.P. McMaster, "Copolymers, polyblends and composites", Chapter 5 in: "Aspects of Liquid-Liquid Phase Transition Phenomena in Multicomponent Polymeric Systems". Advances in Chemistry Series, 142, 1975.

40. J.W. Cahn, J. Chem. Phys. 42, 93 (1965).

41. J.J. van Aartsen and C.A.Smolders, Europ. Polymer J. 6, 1105 (1970).

References (cont.)

42. W.C. Stewart, R.S. Mezrich, L.S. Cosentino, E.M. Nagle, F.S. Wendt and R.D. Lohman, RCA Review $\underline{34}$, 3 (1973).

43. P.F. Gray and H.E. Barnett, Optics Communications $\underline{12}$, 275, (1974).

44. From - Pressure Chemical Co., Pittsburgh, Pa. 15201, U.S.A.

45. From - Hercules, B.V., The Hague, Holland.

46. Y. Katzir, A.A. Friesem and Z. Rav-Noy, in Applications of Holography and Optical Data Processing, Pergamon Press, Oxford, England, 1977.